Among these, *Mat1a* knockout mice have been reported to be hypersensitive to oxidative stress and developed steatosis and HCC.[30] Furthermore, reduced expression of *Gjb2* (*Cx26*) is known to contribute to the promotion and progression of hepatocarcinogenesis in rats.[31]

Of interest, our microarray analysis unveiled the altered expression of genes involved in Wnt/β-catenin signaling; down-regulation of the Wnt antagonist *Sox17* ($P = 0.009$), up-regulation of a Wnt downstream effector *Cyclin D1* ($P = 0.001$), and modestly increased expression of the Wnt receptor *Fzd7* ($P = 0.098$). Wnt/β-catenin signaling is integrally associated with the regulation of stem cells and development of cancer[32] and activated Wnt/β-catenin signaling promotes the proliferation and transformation of hepatic stem/progenitor cells.[3] Together, these results imply that enforced expression of *Bmi1* results in an enhancement of stemness features and the acquisition of malignant potential in normal hepatic stem/progenitor cells, at least in part, through the activation of Wnt signaling. However, further analysis would be necessary to elucidate the relationship between Bmi1 and Wnt signaling.

Surprisingly but importantly, none of the 75 down-regulated genes following *Bmi1*-overexpression was included among the 305 up-regulated genes in neural progenitor cells after *Bmi1* knockdown.[27] Likewise, there existed no overlapping genes between the current expression profile and the 101 commonly regulated genes following *BMI1* knockdown between medulloblastoma and Ewing sarcoma cells.[33,34] In contrast, we detected several genes down-regulated following *Bmi1*-overexpression in hepatic stem/progenitor cells which are also regulated by Bmi1 in hematopoietic stem/progenitor cells (data not shown). These findings support the fact that PcG proteins function in a cell type-specific manner and the composition of PcG complexes is highly dynamic and differs in different cell-types and even at different gene loci.[35]

A comparison of the down-regulated genes with the ChIP-on-chip data for PcG complexes in ESCs revealed five genes that are regulated by PRC1 in ESCs as potential direct targets of Bmi1 in hepatic stem/progenitor cells (Fig. 6B). One of these genes, *Sox17*, is an endodermal marker gene and *Sox17*$^{-/-}$ mice die in the embryonic stage because the endoderm fails to form properly.[22] Therefore, its role in hepatic stem cells remained obscure. In the present study, self-renewal capacity of hepatic stem cells was inversely correlated with the *Sox17* expression levels. Furthermore, cotransduction of *Sox17* with *Bmi1* repressed tumorigenic capacity of Bmi1 in NOD/SCID mice. These findings suggest that Sox17 acts as a tumor suppressor in a specific type of tumor originating from hepatic stem cells. The finding that it is transcriptionally silenced by DNA methylation in human colon cancer cells further supports its role as a tumor suppressor gene.[36] On the other hand, *Sox17*-knockdown in Dlk$^+$ cells alone did not promote tumor initiation in immunodeficient mice. Tumor initiation usually requires multiple steps including activation of oncogenes and repression of tumor suppressor genes. As a number of candidate genes of Bmi1 were identified in this study, coordinated regulation of multiple Bmi1 targets might be needed to recapitulate Bmi1-mediated tumorigenesis *in vivo*. In this regard, knockdown of *Sox17* or other candidate target genes in *Ink4a/Arf*$^{-/-}$ Dlk$^+$ cells would be intriguing to assess for their tumorigenic activity *in vivo*.

Finally, our findings demonstrated that Bmi1 regulates the self-renewal of hepatic stem/progenitor cells to a large extent through the suppression of *Ink4a/Arf*. However, it is evident that targets of Bmi1 other than the *Ink4a/Arf* locus are also responsible for the development of cancer. Further analyses are necessary to determine the roles of the genes listed here in liver development, regeneration, and cancer.

Acknowledgment: The authors thank Dr. M. van Lohuizen for *Bmi1*$^{+/-}$ mice, Dr. W. Pear for the MIGR1 vector, Dr. Valentina M. Factor for the anti-A6 antibody, Dr. N. Nozaki for the anti-Bmi1 antibody, Dr. A. Miyawaki for Kusabira orange, Y. Yamazaki for technical support with the flow cytometry, and M. Tanemura for laboratory assistance.

References

1. Valk-Lingbeek ME, Bruggeman SWM, van Lohuizen M. Stem cells and cancer: the polycomb connection. Cell 2004;118:409-418.
2. Sparmann A, van Lohuizen M. Polycomb silencers control cell fate, development and cancer. Nat Rev Cancer 2006;6:846-856.
3. Chiba T, Zheng YW, Kita K, Yokosuka O, Saisho H, Onodera M, et al. Enhanced self-renewal capability in hepatic stem/progenitor cells drives cancer initiation. Gastroenterology 2007;133:937-950.
4. Mishra L, Banker T, Murray J, Byers S, Thenappan A, He AR, et al. Liver stem cells and hepatocellular carcinoma. HEPATOLOGY 2009;49:318-329.
5. Lessard J, Sauvageau G. Bmi-1 determines the proliferative capacity of normal and leukaemic stem cells. Nature 2003;423:255-260.
6. Leung C, Lingbeek M, Shakhova O, Liu J, Tanger E, Saremaslani P, et al. Bmi1 is essential for cerebellar development and is overexpressed in human medulloblastomas. Nature 2004;428:337-341.
7. Pardal R, Clarke MF, Morrison SJ. Applying the principles of stem-cell biology to cancer. Nat Rev Cancer 2003;3:895-902.
8. Jamieson CH, Weissman IL, Passegue E. Chronic versus acute myelogenous leukemia: a question of self-renewal. Cancer Cell 2004;6:531-533.

9. Park IK, Morrison SJ, Clarke MF. Bmi1, stem cells, and senescence regulation. J Clin Invest 2004;113:175-179.
10. Iwama A, Oguro H, Negishi M, Kato Y, Morita Y, Tsukui H, et al. Enhanced self-renewal of hematopoietic stem cells mediated by the polycomb gene product Bmi-1. Immunity 2004;21:843-851.
11. Oguro H, Iwama A, Morita Y, Kamijo T, van Lohuizen M, Nakauchi H. Differential impact of Ink4a and Arf on hematopoietic stem cells and their bone marrow microenvironment in Bmi1-deficient mice. J Exp Med 2006;203:2247-2253.
12. Molofsky AV, He S, Bydon M, Morrison SJ, Pardal R. Bmi-1 promotes neural stem cell self-renewal and neural development but not mouse growth and survival by repressing the p16Ink4a and p19Arf senescence pathways. Genes Dev 2005;19:1432-1437.
13. Sasaki M, Ikeda H, Itatsu K, Yamaguchi J, Sawada S, Minato H, et al. The overexpression of polycomb group proteins Bmi1 and EZH2 is associated with the progression and aggressive biological behavior of hepatocellular carcinoma. Lab Invest 2008;88:873-882.
14. Tannapfel A, Busse C, Weinans L, Benicke M, Katalinic A, Geissler F, et al. INK4a-ARF alterations and p53 mutations in hepatocellular carcinomas. Oncogene 2001;20:7104-7109.
15. van der Lugt NM, Domen J, Linders K, van Roon M, Robanus-Maandag E, te Riele H, et al. Posterior transformation, neurological abnormalities, and severe hematopoietic defects in mice with a targeted deletion of the bmi-1 proto-oncogene. Genes Dev 1994;8:757-769.
16. Oertel M, Menthena A, Dabeva MD, Shafritz DA. Cell competition leads to a high level of normal liver reconstitution by transplanted fetal liver stem/progenitor cells. Gastroenterology 2006;130:507-520.
17. Dabeva MD, Petkov PM, Sandhu J, Oren R, Laconi E, Hurston E, et al. Proliferation and differentiation of fetal liver epithelial progenitor cells after transplantation into adult rat liver. Am J Pathol 2000;156:2017-2031.
18. Wang X, Foster M, Al-Dhalimy M, Lagasse E, Finegold M, Grompe M. The origin and liver repopulating capacity of murine oval cells. Proc Natl Acad Sci U S A 2003;100(Suppl. 1):11881-11888.
19. Boyer LA, Plath K, Zeitlinger J, Brambrink T, Medeiros LA, Lee TI, et al. Polycomb complexes repress developmental regulators in murine embryonic stem cells. Nature 2006;441:349-353.
20. Lee TI, Jenner RG, Boyer LA, Guenther MG, Levine SS, Kumar RM, et al. Control of developmental regulators by Polycomb in human embryonic stem cells. Cell 2006;125:301-313.
21. Bernstein BE, Mikkelsen TS, Xie X, Kamal M, Huebert DJ, Cuff J, et al. A bivalent chromatin structure marks key developmental genes in embryonic stem cells. Cell 2006;125:315-326.
22. Kanai-Azuma M, Kanai Y, Gad JM, Tajima Y, Taya C, Kurohmaru M, et al. Depletion of definitive gut endoderm in Sox17-null mutant mice. Development 2002;129:2367-2379.
23. Cho CH, Parashurama N, Park EY, Suganuma K, Nahmias Y, Park J, et al. Homogeneous differentiation of hepatocyte-like cells from embryonic stem cells: applications for the treatment of liver failure. FASEB J 2008;22:898-909.
24. Gil J, Peters G. Regulation of the INK4b-ARF-INK4a tumour suppressor locus: all for one or one for all. Nat Rev Mol Cell Biol 2006;7:667-677.
25. Akasaka T, van Lohuizen M, van der Lugt N, Mizutani-Koseki Y, Kanno M, Taniguchi M, et al. Mice doubly deficient for the Polycomb Group genes Mel18 and Bmi1 reveal synergy and requirement for maintenance but not initiation of Hox gene expression. Development 2001;128:1587-1597.
26. Dovey JS, Zacharek SJ, Kim CF, Lees JA. Bmi1 is critical for lung tumorigenesis and bronchioalveolar stem cell expansion. Proc Natl Acad Sci U S A 2008;105:11857-11862.
27. Fasano CA, Dimos JT, Ivanova NB, Lowry N, Lemischka IR, Temple S. shRNA knockdown of Bmi-1 reveals a critical role for p21-Rb pathway in NSC self-renewal during development. Cell Stem Cell 2007;1:87-99.
28. Bruggeman SW, Hulsman D, Tanger E, Buckle T, Blom M, Zevenhoven J, et al. Bmi1 controls tumor development in an Ink4a/Arf-independent manner in a mouse model for glioma. Cancer Cell 2007;12:328-341.
29. Serrano M, Lee H, Chin L, Cordon-Cardo C, Beach D, DePinho RA. Role of the *INK4a* locus in tumor suppression and cell mortality. Cell 1996;85:27-37.
30. Lu SC, Alvarez L, Huang ZZ, Chen L, An W, Corrales FJ, et al. Methionine adenosyltransferase 1A knockout mice are predisposed to liver injury and exhibit increased expression of genes involved in proliferation. Proc Natl Acad Sci U S A 2001;98:5560-5565.
31. Sakamoto H, Oyamada M, Enomoto K, Mori M. Differential changes in expression of gap junction proteins connexin 26 and 32 during hepatocarcinogenesis in rats. Jpn J Cancer Res 1992;83:1210-1215.
32. Reya T, Clevers H. Wnt singnaling in stem cells and cancer. Nature 2005;434:843-850.
33. Wiederschain D, Chen L, Johnson B, Bettano K, Jackson D, Taraszka J, et al. Contribution of polycomb homologues Bmi-1 and Mel-18 to medulloblastoma pathogenesis. Mol Cell Biol 2007;27:4968-4979.
34. Douglas D, Hsu JH, Hung L, Cooper A, Abdueva D, van Doorninck J, et al. BMI-1 promotes ewing sarcoma tumorigenicity independent of CDKN2A repression. Cancer Res 2008;68:6507-6515.
35. Orland V. Polycomb, epigenomes, and control of cell identity. Cell 2003;112:599-606.
36. Zhang W, Glöckner SC, Guo M, Machida EO, Wang DH, Easwaran H, et al. Epigenetic inactivation of the canonical Wnt antagonist SRY-box containing gene 17 in colorectal cancer. Cancer Res 2008;68:2764-2772.

Radiotherapy and Oncology 96 (2010) 231–235

Contents lists available at ScienceDirect

Radiotherapy and Oncology

journal homepage: www.thegreenjournal.com

Particle beam radiotherapy

Comparison of efficacy and toxicity of short-course carbon ion radiotherapy for hepatocellular carcinoma depending on their proximity to the porta hepatis

Hiroshi Imada [a,b,*], Hirotoshi Kato [a], Shigeo Yasuda [a], Shigeru Yamada [a], Takeshi Yanagi [a], Riwa Kishimoto [a], Susumu Kandatsu [a], Jun-etsu Mizoe [a], Tadashi Kamada [a], Osamu Yokosuka [b], Hirohiko Tsujii [a]

[a] National Institute of Radiological Sciences, Chiba, Japan; [b] Department of Medicine and Clinical Oncology, Chiba University, Japan

ARTICLE INFO

Article history:
Received 27 April 2009
Received in revised form 4 March 2010
Accepted 21 May 2010
Available online 25 June 2010

Keywords:
Radiotherapy
Carbon ion
Hepatocellular carcinoma
Porta hepatis

ABSTRACT

Background and purpose: To compare the efficacy and toxicity of short-course carbon ion radiotherapy (C-ion RT) for patients with hepatocellular carcinoma (HCC) in terms of tumor location: adjacent to the porta hepatis or not.

Materials and methods: The study consisted of 64 patients undergoing C-ion RT of 52.8 GyE in four fractions between April 2000 and March 2003. Of these patients, 18 had HCC located within 2 cm of the main portal vein (porta hepatis group) and 46 patients had HCC far from the porta hepatis (non-porta hepatis group). We compared local control, survival, and adverse events between the two groups.

Results: The 5-year overall survival and local control rates were 22.2% and 87.8% in the porta hepatis group and 34.8% and 95.7% in the non-porta hepatis group, respectively. There were no significant differences ($P = 0.252$, $P = 0.306$, respectively). Further, there were no significant differences in toxicities. Biliary stricture associated with C-ion RT did not occur.

Conclusions: Excellent local control was obtained independent of tumor location. The short-course C-ion RT of 52.8 GyE in four fractions appears to be an effective and safe treatment modality in the porta hepatis group just as in the non-porta hepatis group.

 Radiotherapy and Oncology 96 (2010) 231–235

Hepatocellular carcinoma (HCC) is one of the most common malignant tumors worldwide and is the third leading cause of death from cancer [1]. Various therapeutic options are presently available for patients with HCC. In radiotherapy, the role for patients with HCC was previously limited and unsatisfactory on the basis of its poor hepatic tolerance to irradiation [2,3]. Technological advances have made it possible to deliver a higher dose of radiation to focal liver tumors accurately, reducing the degree of toxicity [4–7]. Proton beam therapy was shown to be effective and safe for HCC, mainly due to its excellent dose distribution at the end of the beam path, called the Bragg peak [8–10]. Carbon ion beams also possess the Bragg peak, and they provide excellent dose distribution to the target volume by specified beam modulations [11–15]. They have advantageous biological and physical properties that result in a higher cytocidal effect than that of photons and protons [16–19]. Since 1995, carbon ion radiotherapy (C-ion RT) has been performed for treatment of HCC, and clinical trials were initiated at the National Institute of Radiological Sciences (NIRS).

In terms of HCC adjacent to the porta hepatis, treatment with minimal invasiveness and complications is an important issue. Surgical resection is the standard of curative treatment, but it is restricted to selected patients due to degradation of hepatic function [20,21]. Liver transplantation is a curative treatment of HCC, but it is often not feasible [22–24] and a shortage of donors also limits its possibilities. Radiofrequency ablation (RFA) and other ablative techniques obtain excellent local control, but are limited largely to small HCCs [25–27]. In the presence of blood vessels contiguous with tumor, blood flow reduces the thermal effects of RFA [28–30]. In addition, biliary complications after RFA for HCC adjacent to the porta hepatis sometimes occur, resulting in septic complications and liver failure [31].

We have already reported that C-ion RT used for the treatment of HCC is safe and effective [17,19]. In this study, patients were stratified into two groups according to tumor localization: adjacent to the porta hepatis or not. We compared the treatment effect and toxicity between the two groups retrospectively.

Materials and methods

Patients

Between April 2000 and March 2003, 64 patients with HCC underwent 52.8 GyE/4-fraction C-ion RT in a phase I/II clinical trial or phase II clinical trial at NIRS. The phase I/II clinical trial was carried out from April 2000 to March 2001, and the phase II clinical

* Corresponding author. Address: Research Center for Charged Particle Therapy, National Institute of Radiological Sciences, 4-9-1, Anagawa, Inage-ku, Chiba 263-8555, Japan.
E-mail address: h_imada@nirs.go.jp (H. Imada).

0167-8140/$ - see front matter © 2010 Elsevier Ireland Ltd. All rights reserved.
doi:10.1016/j.radonc.2010.05.019

Table 1
Patient and tumor characteristics.

	Total	Porta hepatis group	Non-porta hepatis group	*P*
N	64	18	46	
Gender, *n* (%)				>0.999
Male	48 (75)	14 (78)	34 (74)	
Female	16 (25)	4 (22)	12 (26)	
Age (years)				0.736
Median	69	68	69	
Range	37–84	51–79	37–84	
Child-Pugh classification, *n* (%)				0.198
A	49 (77)	16 (89)	33 (72)	
B	15 (23)	2 (11)	13 (28)	
Stage (UICC 5th), *n* (%)				0.438
II	23 (36)	5 (28)	18 (39)	
IIIA	32 (50)	9 (50)	23 (50)	
IVA	9 (14)	4 (22)	5 (11)	
Maximum tumor diameter (mm)				0.725
Median	40.0	36.5	40.0	
Range	12–120	21–120	12–112	
Vascular invasion				0.066
Yes	45 (70)	16 (89)	29 (63)	
No	19 (30)	2 (11)	17 (37)	
Number of tumors, *n* (%)				0.676
Single	56 (88)	15 (83)	41 (89)	
Multiple	8 (12)	3 (17)	5 (11)	

Abbreviations: UICC = International Union against cancer.

trial was sequentially performed from April 2001 to March 2003. The eligibility criteria were previously reported [17]. HCC was diagnosed by needle biopsy in all patients. Prior to treatment, all patients gave their informed consent in writing in accordance with the Declaration of Helsinki. These clinical trials were approved by the ethics committees at NIRS. Eighteen of the 64 patients had HCC located within 2 cm from the main portal vein, and the other 46 had HCC far from the porta hepatis.

Background data of the patients and tumors are presented in Table 1. The enrolled patients consisted of 48 males and 16 females. Median age was 69 years (range, 37–84). Child-Pugh classification of the degree of liver impairment was as follows: 49 patients were categorized as Class A (scores, 5–6), and 15 patients as Class B (scores, 7–9). Twenty-three patients had Stage II, 32 had Stage IIIA, and 9 had Stage IVA. By the Barcelona Clinic Liver Cancer staging classification [32,33], 2 patients had Stage A and 16 had Stage C in the porta hepatis group, and 15 had Stage A, 2 had Stage B, and 29 had Stage C in the non-porta hepatis group. Median maximum tumor diameter was 40 mm (range, 12–120). Forty-five patients had vascular invasion. Fifty-six patients had a solitary mass and 8 had multiple tumors.

Pretreatment evaluation

Laboratory values collected for all patients included complete blood cell counts, liver and renal function tests, electrolytes, HBV and HCV titers, and α-fetoprotein (AFP). Abdominal triphasic CT or MRI was performed for evaluation of the extent of HCC.

C-ion RT

The carbon ion beam used for radiotherapy was generated by the heavy ion medical accelerator in Chiba developed by NIRS in 1993. The accelerator system and the biophysical characteristics of the carbon ion beam have been previously described [13–15]. For modulation of the Bragg peak of the beam to conform to the target volume, the beam lines in the treatment room are equipped with a pair of wobbler magnets, beam scatterers, ridge filters, multileaf collimators, and a compensation bolus.

Before therapeutic planning, all patients had metallic markers (iridium seeds, 0.5 mm in diameter and 3 mm in length) implanted near the tumor to obtain precise treatment positioning. The irradiation fields were established with a three-dimensional therapy plan on the basis of 5-mm-thick CT images. The planning target volume was defined according to the shape of the tumor plus a 1.0–1.2 cm margin. To reproduce the target position accurately, a low-temperature thermoplastic sheet (Shellfitter, Kuraray, Osaka, Japan), a customized cradle (Moldcare, Alcare, Tokyo, Japan), and a respiratory gated irradiation system [34] were used in the CT planning and radiotherapy performance. The radiation field was confirmed and corrected by orthogonal fluoroscopy and radiography immediately before each treatment session.

Irradiation doses were expressed in Gray equivalents (GyE = carbon physical dose [in Gray] × relative biologic effectiveness). The relative biologic effectiveness value of carbon ions was assumed to be 3 at the distal part of the spread-out Bragg peak [35]. C-ion RT was given once daily, 4 days a week, for four fractions in 1 week. The dose per fraction was 13.2 GyE, so all patients received a total dose of 52.8 GyE.

Follow-up and evaluation criteria

All patients were assessed according to a predetermined schedule. After C-ion RT, patients were evaluated on the basis of physical examinations and blood tests once a month for the first year, once every 3 months for the following year, and once every 3–6 months thereafter. Contrast-enhanced CT or MRI was performed every 3 months for the first 2 years and every 6 months thereafter. Local control was defined as no sign of regrowth or new tumor in the treatment volume. Local recurrence was defined as failure of local control. Overall survival was measured from the starting date of treatment until the date of death from any cause. Cause-specific survival was defined as the interval between the starting date of treatment and the date of death from liver failure or HCC. Disease-free survival was defined as the interval between the starting date of treatment and the date of the diagnosis of the first recurrence or death from any cause. Acute and late toxicities were assessed using the National Cancer Institute Common Criteria, version 2.0, and the Radiation Therapy Oncology Group/European Organization for Research and Treatment of Cancer late radiation morbidity scoring scheme. Liver toxicity in late phase was assessed by Child-Pugh score, a commonly used marker of hepatic functional reserve in chronic liver disease.

Statistical analysis

Statistical analyses were performed using SPSS version 12.0 (SPSS Inc., Chicago, IL). For continuous variables, non-parametric tests (Mann–Whitney *U* test) were used. For categorical data, chi-squared test or Fisher's exact test was used. The Kaplan–Meier method was used for calculation of local control and survival rates, and the survival curves were compared by log-rank test. Statistical significance was considered if $P < 0.05$ (*P*-values from two-sided tests).

Results

There were no significant differences in sex, age, Child-Pugh classification, clinical stage, maximum tumor diameter, and tumor number between the two groups. The porta hepatis group exhibited greater vascular invasion than the non-porta hepatis group ($P = 0.066$).

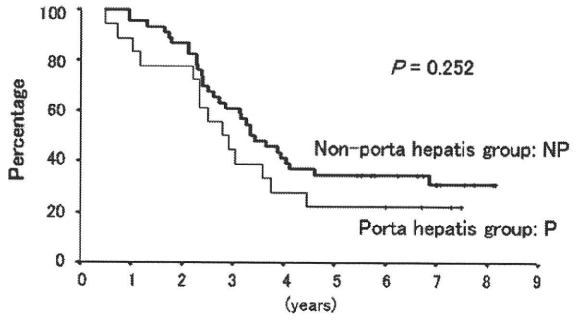

Number of patients at risk

NP	46	44	40	28	19	16	12	7	2	0
P	18	16	14	8	5	4	4	2	0	0

Fig. 1. Overall survival rate according to tumor localization. Overall survival rates after 3 and 5 years were 44.4% and 22.2% in the porta hepatis group and 60.9% and 34.8% in the non-porta hepatis group, respectively. There were no significant differences between the two groups ($P = 0.252$).

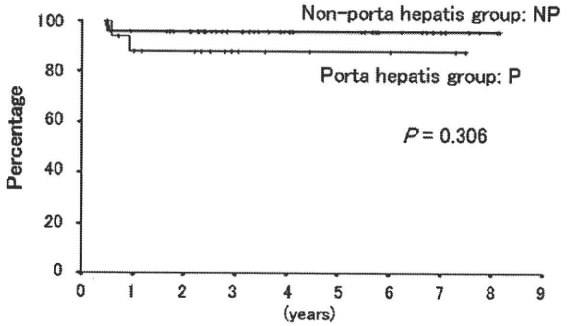

Number of patients at risk

NP	46	42	39	28	19	16	12	7	2	0
P	18	14	12	6	4	3	3	2	0	0

Fig. 2. Local control rate according to tumor localization. Local control rates after both 3 and 5 years were 87.8% in the porta hepatis group and 95.7% in the non-porta hepatis group. There were no significant differences between the two groups ($P = 0.306$).

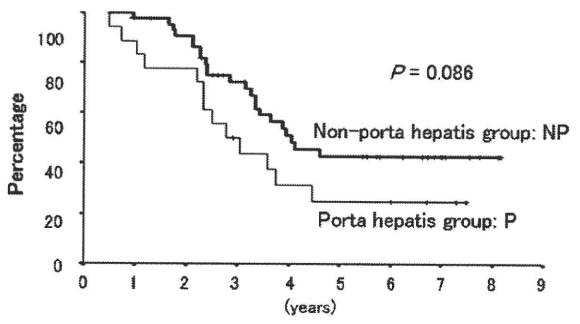

Number of patients at risk

NP	46	44	40	28	19	16	12	7	2	0
P	18	16	14	8	5	4	4	2	0	0

Fig. 3. Cause-specific survival rate according to tumor localization. Cause-specific survival rates after 3 and 5 years were 50.0% and 25.0% in the porta hepatis group and 72.3% and 42.8% in the non-porta hepatis group, respectively. The porta hepatis group showed a trend towards inferior outcome compared to the non-porta hepatis group ($P = 0.086$).

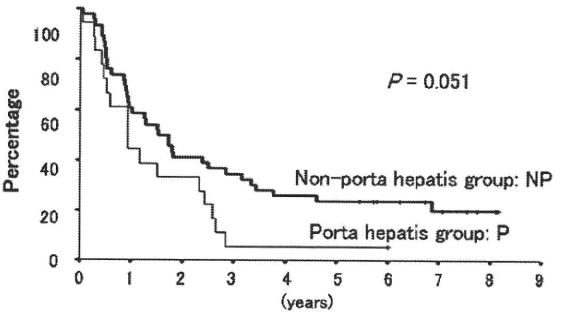

Number of patients at risk

NP	46	28	19	16	12	11	8	5	2	0
P	18	8	6	1	1	1	1	0	0	0

Fig. 4. Disease-free survival rate according to tumor localization. Disease-free survival rates after both 3 and 5 years were 5.6% in the porta hepatis group, and they were 34.8% and 23.9% in the non-porta hepatis group, respectively. The porta hepatis group showed a trend towards inferior outcome compared to the non-porta hepatis group ($P = 0.051$).

The median observation period for survival was 34 months (range, 6–90 months) in the porta hepatis group and 41 months (range, 11–98 months) in the non-porta hepatis group. Four patients were alive at last follow-up and 14 had died in the porta hepatis group, and 15 were alive at last follow-up and 31 had died in the non-porta hepatis group. Overall survival rates after 3 and 5 years were 44.4% [95% confidence interval (CI), 22–67] and 22.2% [95% CI, 3–41] in the porta hepatis group and 60.9% [95% CI, 47–75] and 34.8% [95% CI, 21–49] in the non-porta hepatis group, respectively (Fig. 1). Local control rates after both 3 and 5 years were 87.8% [95% CI, 72–104] in the porta hepatis group and 95.7% [95% CI, 90–102] in the non-porta hepatis group, respectively (Fig. 2). There were no significant differences between the two groups in overall survival and local control rates ($P = 0.252$, $P = 0.306$, respectively). Cause-specific survival rates after 3 and 5 years were 50.0% [95% CI, 27–73] and 25.0% [95% CI, 4–46] in the porta hepatis group and 72.3% [95% CI, 59–86] and 42.8% [95% CI, 27–58] in the non-porta hepatis group, respectively (Fig. 3). Disease-free survival rates after both 3 and 5 years were 5.6% [95% CI, −5 to 16] in the porta hepatis group, and they were 34.8% [95% CI, 21–49] and 23.9% [95% CI, 12–36] in the non-porta hepatis group, respectively (Fig. 4). In the cause-specific and disease-free survival rates, the porta hepatis group showed a trend towards inferior outcome compared to the non-porta hepatis group ($P = 0.086$, $P = 0.051$, respectively).

Toxicities in early phase are shown in Table 2. Adverse events of grade 3 or more were compared between the two groups. There were no significant differences in hepatic and hematologic toxicities ($P > 0.999$, $P = 0.190$, respectively). As to Child-Pugh score in late phase, cases with changes in Child-Pugh score within 1-point increase were 13 in the porta hepatis group and 41 in the non-porta hepatis group. Those with changes in score increasing by at least 2 points were five in each of the groups. There were no significant differences between the two groups in terms of change in Child-Pugh score (≤ 1 vs. ≥ 2) ($P = 0.128$) (Table 3). In terms of other non-hematologic toxicities such as skin and gastrointestinal toxicities, toxicities of grade 3 or higher did not occur. No patient had biliary stenosis associated with C-ion RT.

Table 2
Toxicities in early phase.

	Porta hepatis group Grade					Non-porta hepatis group Grade				
	0	1	2	3	4	0	1	2	3	4
Liver	2	4	9	3	0	7	15	16	8	0
Blood	6	2	4	6	0	13	9	16	8	0

There were no significant differences between porta hepatis and non-porta hepatis groups in liver and blood toxicities (grade 0–2 vs. grade 3–4) by Fisher's exact test. $P > 0.999$ (liver toxicity); $P = 0.190$ (blood toxicity).

Table 3
Change of Child-Pugh score in late phase.

	≦1	≧2
Porta hepatis group	13	5
Non-porta hepatis group	41	5

There were no significant differences between porta hepatis and non-porta hepatis groups in change of Child-Pugh score (≦1 vs. ≧2) by Fisher's exact test. $P = 0.128$.

Discussion

It is important that the treatment of HCC involves minimum invasiveness and complications in general. Surgical resection and RFA are essential curative therapies for HCC. In surgical resection, it was reported that both the 5-year overall survival and disease-free survival rates of the anatomic resection group were significantly better than those of the non-anatomic resection group, as HCC has a nature to cause intrahepatic metastasis via vascular invasion [36]. Anatomic resection consists of the systematic removal of a hepatic segment confined by tumor-bearing portal tributaries. In some patients with HCC adjacent to the porta hepatis, anatomic resection implies greater invasiveness because the resection volume becomes larger.

Concerning the use of RFA, puncture of the liver hilus, with the risk of injury to the portal vein or bile duct, presents a potentially dangerous scenario. It was reported that RFA was performed for patients with HCC adjacent to the porta hepatis under the condition of cooling the bile duct by endoscopic nasobiliary drainage tube to prevent biliary complications [31]. But the procedure is too complex to be a common therapy. Additionally, in cases of HCC with contiguous vessels, blood flow reduces the thermal effects of RFA, a phenomenon that increases the likelihood of the presence of residual viable tumor cells [37–39].

According to the above, we need to consider the degree of invasiveness and complications and carefully select an appropriate treatment modality because HCC adjacent to the porta hepatis is close to vessels and bile duct. In this study, therefore, differences in treatment effect and toxicities according to tumor localization, whether adjacent to the porta hepatis or not, were investigated retrospectively.

In the comparison of patient and tumor characteristics, the porta hepatis group demonstrated a trend towards a higher rate of vascular invasion compared to the non-porta hepatis group ($P = 0.066$). It is suggested that this was due to the tumor location.

Local control rates after 5 years were 87.8% [95% CI, 72–104] in the porta hepatis group and 95.7% [95% CI, 90–102] in the non-porta hepatis group. Thus, we obtained excellent local control rates in both groups. Local failure occurred in only four of all patients—two each in the porta hepatis and non-porta hepatis groups. There were no significant differences in toxicities. Biliary stenosis associated with C-ion RT did not occur in either group. Therefore, in certain patients with a higher risk of injury to the bile duct when undergoing RFA, in high-risk cases such as elderly patients for postoperative complications after surgical resection, or in some patients who refuse to undergo hepatectomy or RFA, C-ion RT appears to offer a promising therapeutic alternative for HCC.

However, cause-specific and disease-free survival rates after 5 years were 25.0% [95% CI, 4–46] and 5.6% [95% CI, −5 to 16] in the porta hepatis group and 42.8% [95% CI, 27–58] and 23.9% [95% CI, 12–36] in the non-porta hepatis group, respectively, which indicates a difference which is of borderline significance ($P = 0.086$, $P = 0.051$). The presence of vascular invasion is higher in the porta hepatis group ($P = 0.066$). A characteristic of HCC is the potential of causing intrahepatic metastasis via vascular invasion, and therefore the cause-specific and disease-free survival rates are mainly representing the rate of intrahepatic metastases/new tumors as there were almost no local failures (Fig. 2). This emphasizes the necessity to take into account the possibility of intrahepatic metastasis via vascular invasion. Of course, the importance of the earliest possible detection of a new tumor lesion and its treatment with an appropriate therapeutic modality cannot be overstated. In this regard, it is considered especially important to keep in mind the clinical multidisciplinary approach available for treating HCC.

As for radiation therapy for HCC adjacent to the porta hepatis, it was reported that proton beam therapy delivering 72.6 GyE in 22 fractions appears effective and safe. Overall 3-year survival and local control rates were 45.1% and 86.0%, respectively [40]. In our study, these rates in the porta hepatis group were 44.4% [95% CI, 22–67] and 87.8% [95% CI, 72–104], respectively. Therefore, the treatment effect of short-course C-ion RT is suggested to be almost equal to that of proton beam therapy with a more fractionated regimen.

A limitation of this study was the fact that the patient number in the porta hepatis group was small. It is therefore important to collect such cases and continuously verify efficacy and safety of short-course C-ion RT for patients with HCC adjacent to the porta hepatis.

In conclusion, excellent local control was achieved independent of tumor localization. There was no significant difference in treatment-related toxicity between the porta hepatis and non-porta hepatis groups. The short-course C-ion RT of 52.8 GyE in four fractions appears to be an effective and safe therapeutic option for porta hepatis patients just as it is for non-porta hepatis patients.

Conflict of interest statement

Any actual or potential conflicts of interest do not exist.

Acknowledgements

This study was supported by the Research Project with Heavy Ions of the National Institute of Radiological Sciences in Japan. We are grateful to the members of the National Institute of Radiological Sciences.

References

[1] Bosch FX, Ribes J, Borras J. Epidemiology of primary liver cancer. Semin Liver Dis 1999;19:271–85.
[2] Phillips R, Murakami K. Preliminary neoplasms of the liver. Results of radiation therapy. Cancer 1960;13:714–20.
[3] Stillwagon GB, Order SE, Guse C, et al. 194 Hepatocellular cancers treated by radiation and chemotherapy combinations: Toxicity and response: a Radiation Therapy Oncology Group study. Int J Radiat Oncol Biol Phys 1989;17:1223–9.
[4] Robertson JM, Lawrence TS, Dworzanin LM, et al. Treatment of primary hepatobiliary cancers with conformal radiation therapy and regional chemotherapy. J Clin Oncol 1993;11:1286–93.
[5] Toya R, Murakami R, Baba Y, et al. Conformal radiation therapy for portal vein tumor thrombosis of hepatocellular carcinoma. Radiother Oncol 2007;84:266–71.

[6] Xi M, Liu MZ, Deng XW, et al. Defining internal target volume (ITV) for hepatocellular carcinoma using four-dimensional CT. Radiother Oncol 2007;84:272–8.
[7] Zhao JD, Xu ZY, Zhu J, et al. Application of active breathing control in 3-dimensional conformal radiation therapy for hepatocellular carcinoma: the feasibility and benefit. Radiother Oncol 2008;87:439–44.
[8] Suit HD, Goitein M, Munzenrider J, et al. Increased efficacy of radiation therapy by use of proton beam. Strahlenther Onkol 1990;166:40–4.
[9] Matsuzaki Y, Osuga T, Saito Y, et al. A new, effective, and safe therapeutic option using proton irradiation for hepatocellular carcinoma. Gastroenterology 1994;106:1032–41.
[10] Matsuzaki Y. The efficacy of powerful proton radiotherapy for hepatocellular carcinoma-long term effects and QOL. Ann Cancer Res Ther 1998;7:9–17.
[11] Blakely EA, Ngo FQH, Curtis SB, et al. Heavy ion radiobiology: cellular studies. Adv Radiat Biol 1984;11:295–378.
[12] Castro JR. Future research strategy for heavy ion radiotherapy. In: Kogelnih HD, editor. Progress in radio-oncology. Bologna: Monduzzi Editore; 1995. p. 643–8.
[13] Sato K, Yamada H, Ogawa K, et al. Performance of HIMAC. Nucl Phys 1995;A588:229–34.
[14] Kanai T, Furusawa Y, Fukutsu K, Itsukaichi H, Eguchi-Kasai K, Ohara H. Irradiation of mixed beam and design of spread-out Bragg peak for heavy-ion radiotherapy. Radiat Res 1997;147:78–85.
[15] Kanai T, Endo M, Minohara S, et al. Biophysical characteristics of HIMAC clinical irradiation system for heavy-ion radiation therapy. Int J Radiat Oncol Biol Phys 1999;44:201–10.
[16] Tsujii H, Morita S, Miyamoto T, et al. Preliminary results of phase I/II carbon ion therapy. J Brachyther Int 1997;13:1–8.
[17] Kato H, Tsujii H, Miyamoto T, et al. Results of the first prospective study of carbon ion radiotherapy for hepatocellular carcinoma with liver cirrhosis. Int J Radiat Oncol Biol Phys 2004;59:1468–76.
[18] Tsujii H, Mizoe JE, Kamada T, et al. Overview of clinical experiences on carbon ion radiotherapy at NIRS. Radiother Oncol 2004;73:S41–49.
[19] Kato H, Yamada S, Yasuda S, et al. Phase II study of short-course carbon ion radiotherapy (52.8 GyE/4-fraction/1-week) for hepatocellular carcinoma. Hepatology 2005;42:381A.
[20] Ikai I, Arii S, Okazaki M, et al. Report of the 17th nationwide follow-up survey of primary liver cancer in Japan. Hepatol Res 2007;37:676–91.
[21] Mulcahy MF. Management of hepatocellular cancer. Curr Treat Options Oncol 2005;6:423–35.
[22] Mazzaferro V, Regalia E, Doci R, et al. Liver transplantation for the treatment of small hepatocellular carcinomas in patients with cirrhosis. N Engl J Med 1996;334:693–9.
[23] Llovet JM, Fuster J, Bruix J. Intention-to-treat analysis of surgical treatment for early hepatocellular carcinoma: resection versus transplantation. Hepatology 1999;30:1434–40.
[24] Yoo HY, Patt CH, Geschwind JF, et al. The outcome of liver transplantation in patients with hepatocellular carcinoma in the United States between 1988 and 2001: 5-year survival has improved significantly with time. J Clin Oncol 2003;21:4329–35.
[25] Kuvshinoff BW, Ota DM. Radiofrequency ablation of liver tumors: influence of technique and tumor size. Surgery 2002;132:605–11.
[26] Shiina S, Teratani T, Obi S, et al. A randomized controlled trial of radiofrequency ablation with ethanol injection for small hepatocellular carcinoma. Gastroenterology 2005;129:122–30.
[27] Sato M, Watanabe Y, Ueda S, et al. Microwave coagulation therapy for hepatocellular carcinoma. Gastroenterology 1996;110:1507–14.
[28] Patterson EJ, Scudamore CH, Owen DA, et al. Radiofrequency ablation of porcine liver in vivo: effects of blood flow and treatment time on lesion size. Ann Surg 1998;227:559–65.
[29] Livraghi T, Solbiati L, Meloni MF, et al. Treatment of focal liver tumors with percutaneous radio-frequency ablation: complications encountered in a multicenter study. Radiology 2003;226:441–51.
[30] Nakazawa T, Kokubu S, Shibuya A, et al. Radiofrequency ablation of hepatocellular carcinoma: correlation between local tumor progression after ablation and ablative margin. AJR Am J Roentgenol 2007;188:480–8.
[31] Ohnishi T, Yasuda I, Nishigaki Y, et al. Intraductal chilled saline perfusion to prevent bile duct injury during percutaneous radiofrequency ablation for hepatocellular carcinoma. J Gastroenterol Hepatol 2008;23:e410–415.
[32] Llovet JM, Bru C, Bruix J. Prognosis of hepatocellular carcinoma: the BCLC staging classification. Semin liver Dis 1999;19:329–38.
[33] Llovet JM, Burroughs A, Bruix J. Hepatocellular carcinoma. Lancet 2003;362:1907–17.
[34] Minohara S, Kanai T, Endo M, Noda K, Kanazawa M. Respiratory gated irradiation system for heavy-ion radiotherapy. Int J Radiat Oncol Biol Phys 2000;47:1097–103.
[35] Suzuki M, Kase Y, Yamaguchi H, Kanai T, Ando K. Relative biological effectiveness for cell-killing effect on various human cell lines irradiated with heavy-ion medical accelerator in Chiba (HIMAC) carbon-ion beams. Int J Radiat Oncol Biol Phys 2000;48:241–50.
[36] Hasegawa K, Kokudo N, Imamura H, et al. Prognostic impact of anatomic resection for hepatocellular carcinoma. Ann Surg 2005;242:252–9.
[37] Rossi S, Garbagnati F, Lencioni R, et al. Percutaneous radio-frequency thermal ablation of nonresectable hepatocellular carcinoma after occlusion of tumor blood supply. Radiology 2000;217:119–26.
[38] McGhana JP, Dodd 3rd GD. Radiofrequency ablation of the liver: current status. AJR Am J Roentgenol 2001;176:3–16.
[39] de Baere T, Denys A, Wood BJ, et al. Radiofrequency liver ablation: experimental comparative study of water-cooled versus expandable systems. AJR Am J Roentgenol 2001;176:187–92.
[40] Mizumoto M, Tokuuye K, Sugahara S, et al. Proton beam therapy for hepatocellular carcinoma adjacent to the prota hepatis. Int J Radiat Oncol Biol Phys 2008;71:462–7.

Radiotherapy and Oncology 96 (2010) 236–242

Contents lists available at ScienceDirect

Radiotherapy and Oncology

journal homepage: www.thegreenjournal.com

Particle beam radiotherapy

Compensatory enlargement of the liver after treatment of hepatocellular carcinoma with carbon ion radiotherapy – Relation to prognosis and liver function

Hiroshi Imada [a,b,*], Hirotoshi Kato [a], Shigeo Yasuda [a], Shigeru Yamada [a], Takeshi Yanagi [a], Ryusuke Hara [a], Riwa Kishimoto [a], Susumu Kandatsu [a], Shinichi Minohara [a], Jun-etsu Mizoe [a], Tadashi Kamada [a], Osamu Yokosuka [b], Hirohiko Tsujii [a]

[a] Research Center for Charged Particle Therapy, National Institute of Radiological Sciences, Chiba, Japan; [b] Department of Medicine and Clinical Oncology, Graduate School of Medicine, Chiba University, Chiba, Japan

ARTICLE INFO

Article history:
Received 30 December 2008
Received in revised form 3 December 2009
Accepted 18 March 2010
Available online 21 April 2010

Keywords:
Hepatocellular carcinoma
Radiotherapy
Carbon ion
Liver volume
Liver function

ABSTRACT

Background and purpose: To examine whether liver volume changes affect prognosis and hepatic function in patients treated with carbon ion radiotherapy (CIRT) for hepatocellular carcinoma (HCC).

Material and methods: Between April 1995 and March 2003, among the cases treated with CIRT, 43 patients with HCC limited to the right hepatic lobe were considered eligible for the study. The left lateral segment was defined as the non-irradiated region. Liver volume was measured using contrast CT at 0, 3, 6, and 12 months after CIRT. We examined serum albumin, prothrombin activity, and total bilirubin level as hepatic functional reserve.

Results: After CIRT, the non-irradiated region showed significant enlargement, and enlarged volume of this region 3 months after CIRT $\geqslant 50\ cm^3$ was a prognostic factor. The 5-year overall survival rates were 48.9% in the larger enlargement group (enlarged volume of non-irradiated region 3 months after CIRT $\geqslant 50\ cm^3$) and 29.4% in the smaller enlargement group (as above, $<50\ cm^3$). The larger enlargement group showed better hepatic functional reserve than the smaller enlargement group 12 months after CIRT.

Conclusions: This study suggests that compensatory enlargement in the non-irradiated liver after CIRT contributes to the improvement of prognosis.

 Radiotherapy and Oncology 96 (2010) 236–242

Hepatocellular carcinoma (HCC) is one of the most common malignant tumors in the world and is the third-leading cause of death from cancer [1]. In Japan, its incidence is approximately 30 in 100,000 males and 10 in 100,000 females [2]. HCC is closely associated with hepatitis B and C, and the majority of patients with HCC have liver cirrhosis, a condition that limits treatment options. Surgical resection is the mainstay of curative treatment, but it is restricted to selected patients [3,4]. Radiofrequency ablation and other ablative techniques achieve excellent local control, but they are restricted to small HCC [5–7]. Transcatheter arterial chemoembolization is clinically useful [8–10], but a radical effect has not been proved in histopathologic studies [11,12]. There is an urgent need for more effective and less invasive treatment of HCC.

The previous role of radiotherapy for HCC was limited and unsatisfactory by poor hepatic tolerance to irradiation [13,14]. Technological advances have made it possible to deliver a higher dose of radiation to focal liver cancers accurately, reducing the risk of toxicity [15–17]. Proton beam therapy has appeared to be effective and safe for HCC, mainly because of its excellent dose distribution at the end of the beam path, called the Bragg peak [18,19]. Carbon ion beams also possess the Bragg peak, and they provide excellent dose localization to the target volume by specified beam modulations [20,21]. They have advantageous biological and physical properties that result in a higher cytocidal effect than those of photons and protons [22–27].

The history of the use of carbon ion radiotherapy (CIRT) for treating HCC goes back to 1995, when clinical trials were initiated at the National Institute of Radiological Sciences (NIRS). We have already reported that CIRT used for the treatment of HCC is safe and effective, and that it causes only minor liver damage [22,23]. Although atrophy of the irradiated region of the liver is observed after CIRT, the reason why liver function is retained after CIRT has not yet been investigated.

It has been reported that preoperative portal vein embolization in extended hepatectomy cases causes the remnant liver volume to increase and postoperative hepatic insufficiency to diminish [28,29]. Similarly, we wondered whether the same mechanism might apply to CIRT. Thus, as the region irradiated with CIRT showed atrophy and the non-irradiated region appeared to show

* Corresponding author at: Research Center for Charged Particle Therapy, National Institute of Radiological Sciences, 4-9-1, Anagawa, Inage-ku, Chiba 263-8555, Japan.
E-mail address: h_imada@nirs.go.jp (H. Imada).

0167-8140/$ - see front matter © 2010 Elsevier Ireland Ltd. All rights reserved.
doi:10.1016/j.radonc.2010.03.025

compensatory enlargement after CIRT, it was supposed that the compensatory enlargement had a contributory role in the retention of hepatic function. This hypothesis was investigated.

Materials and methods

Patients

CIRT for HCC was performed as a Phase I/II clinical trial from April 1995 through March 2001 with 110 patients, and as a Phase II clinical trial from April 2001 through March 2003 with 47 patients. The eligibility criteria for enrollment in these clinical trials were previously reported [22]. Prior to treatment, all patients gave their written informed consent in accordance with the Declaration of Helsinki. One hundred twenty-one of the total 157 had the tumor limited to the right lobe of the liver, 27 had the tumor limited to the left lobe, and 9 had the tumor in both right and left lobes.

Among the patients of this study, 43 met the following conditions: (1) treatment target tumor was limited to the right lobe of the liver, (2) left lateral segment was not irradiated, (3) no additional treatment was performed for hepatic lesions (local recurrence and/or recurrence in other loci) within 12 months after CIRT, and (4) abdominal contrast CT imaging was performed at our institute at 0, 3, 6 and 12 months after CIRT. Background data of the patients and tumors are presented in Table 1. The regions irradiated with more than 10% radiation dose were as follows: anterior, posterior and medial segments in 32 patients, anterior and posterior segments in 8, posterior segment in 2, and anterior and medial segments in 1.

Carbon ion radiotherapy

The carbon ion beam used for radiotherapy was generated from the heavy ion medical accelerator in Chiba developed by NIRS in 1993. The accelerator system and the biophysical characteristics of the carbon ion beam have been previously described [20,21,30]. For modulation of the Bragg peak of the beam to conform to the target volume, the beam lines in the treatment room are equipped with a pair of wobbler magnets, beam scatterers, ridge filters, multileaf collimators, and a compensation bolus. The irradiation fields were established with a three-dimensional therapy plan on the basis of 5-mm-thick CT images. The planning target volume was defined according to the shape of the tumor plus a 1.0–1.2 cm margin. To reproduce the target position accurately, a low-temperature thermoplastic sheet (Shellfitter, Kuraray, Osaka, Japan), a customized cradle (Moldcare, Alcare, Tokyo, Japan), and a respiratory gated irradiation system [31] were used in the CT planning and radiotherapy stages. The radiation field was confirmed and corrected by orthogonal fluoroscopy and radiography immediately before each treatment session.

Table 1
Patient and tumor characteristics.

	Total	Larger enlargement group	Smaller enlargement group	*P*
n	43	20	23	
Gender, n (%)				
Male	29 (67)	15 (75)	14 (61)	0.353
Female	14 (33)	5 (25)	9 (39)	
Age (years)				
Median	66	71.5	65	0.006
Range	45–83	46–81	45–83	
Child-Pugh classification, n (%)				
A	35 (81)	18 (90)	17 (74)	0.250
B	8 (19)	2 (10)	6 (26)	
Stage (UICC 5th), n (%)				
I	13 (32)	6 (27)	7 (36)	0.947
II	25 (54)	12 (59)	13 (50)	
IIIA	5 (14)	2 (14)	3 (14)	
Gross tumor volume (cm^3)				
Median	35.2	54.7	31.8	0.114
Range	4.6–861.9	15.6–861.9	4.6–211.2	
Planning target volume (cm^3)				
Median	190.5	242.9	149.0	0.019
Range	39.6–1466.4	70.3–1466.4	39.6–538	
Liver volume of irradiated site (cm^3), mean ± SD	756.6 ± 134.1	767.1 ± 138.1	747.5 ± 132.9	0.942
Liver volume of non-irradiated site (cm^3), mean ± SD	320.0 ± 166.3	317.2 ± 152.7	322.4 ± 180.6	0.715
Albumin (g/dl), mean ± SD	3.8 ± 0.4	3.9 ± 0.4	3.8 ± 0.4	0.659
Prothrombin activity (%), mean ± SD	77.2 ± 13.5	78.6 ± 11.4	76.0 ± 15.3	0.670
Total bilirubin (mg/dl), mean ± SD	1.0 ± 0.4	0.9 ± 0.3	1.1 ± 0.4	0.072
Platelet count ($\times 10^4/\mu l$), mean ± SD	11.8 ± 4.6	14.0 ± 4.3	9.9 ± 3.9	0.002
Number of tumors, n (%)				
1	36 (84)	19 (95)	17 (74)	0.100
2	7 (16)	1 (5)	6 (26)	
Irradiated segment, n (%)				
Anterior, posterior and medial	32	15	17	0.821
Anterior and posterior	8	4	4	
Posterior	2	1	1	
Anterior and medial	1	0	1	
Number of portals, n (%)				
2	36	16	20	0.687
3	7	4	3	

Abbreviations: UICC = International Union Against Cancer.
SD = standard deviation.

Table 2
Dose fractionation.

Total dose/ fractionation	Total (n = 43)	Larger enlargement group (n = 20)	Smaller enlargement group (n = 23)	BED (α/ β = 10)
49.5 GyE/15 fr	1	1	0	65.8
54.0 GyE/15 fr	1	0	1	73.4
60.0 GyE/15 fr	2	0	2	84.0
66.0 GyE/15 fr	2	1	1	95.0
72.0 GyE/15 fr	3	1	2	106.6
79.5 GyE/15 fr	1	0	1	121.6
54.0 GyE/12 fr	1	0	1	78.3
60.0 GyE/12 fr	3	2	1	90.0
66.0 GyE/12 fr	2	2	0	102.3
69.6 GyE/12 fr	4	1	3	110.0
48.0 GyE/8 fr	2	0	2	76.8
52.8 GyE/8 fr	7	3	4	87.6
52.8 GyE/4 fr	14	9	5	122.5

Abbreviations: BED = biological effective dose.

The dose was calculated for the target volume and any nearby critical structures and expressed in Gray equivalents (GyE = carbon physical dose [in Gray] × relative biologic effectiveness). Radiobiologic studies were performed in mice and in five human cell lines cultured *in vitro* to estimate the relative biologic effectiveness values relative to megavoltage photons. Irrespective of the size of the spread-out Bragg peak (SOBP), the relative biologic effectiveness value of carbon ions was estimated as 3.0 at the distal part of the SOBP, and ridge filters were designed to produce a physical dose gradient of the SOBP so that the biologic effect along the SOBP became uniform. This was based on the biologic response of human salivary gland tumor cells at a 10% survival level.

CIRT was given at a total dose range of 48.0–79.5 GyE in 4–15 fractions. Ten patients were treated at a total dose range of 49.5–79.5 GyE in 15 fractions, 10 at 54.0–69.6 GyE in 12 fractions, 9 at 48.0–52.8 GyE in 8 fractions, and 14 at 52.8 GyE in four fractions. CIRT was administered once a day, four fractions per a week, and one port was used in each session. Double-field geometry was used for CIRT in 36 patients; for the remaining seven patients, three-field geometry was used (Tables 1 and 2).

Measurement of liver volume

The left lateral segment of the liver was defined as the non-irradiated region, and the other segments as irradiated. The AZE Company Workstation VIRTUAL PLACE ADVANCE PLUS liver analysis software was used for measuring liver volume. Liver contours (both irradiated and non-irradiated regions) and contours of the target tumors to be treated were entered on each of the CT slices taken prior to treatment and at 3, 6 and 12 months after CIRT, and the volume of the liver in the irradiated region (excluding the target tumor volume) as well as that in the non-irradiated region were measured. Since hepatic cirrhosis is noted in most cases as the background disease, and to exclude any impact of right lobe atrophy and left lobe enlargement through natural processes, the evaluation period was limited to 12 months after treatment.

Survival and evaluation of liver function

Overall survival was measured from the starting date of treatment until the date of death from any cause. Disease-free survival was measured from the starting date of treatment to the time of either death due to disease or of the first clinical or radiographic evidence of systemic or regional disease recurrence. We investigated the relationships between survivals and enlargement volume of the non-irradiated region at 3 months after CIRT. Patients with 50 cm^3 or greater enlargement volume of the non-irradiated region at 3 months post-treatment were classified as the larger enlargement group, and those with less than 50 cm^3 enlargement as the smaller enlargement group. Serial changes in serum albumin, prothrombin activity, total bilirubin level, and platelet count were reviewed before and 12 months after treatment in the larger and smaller enlargement groups.

Statistical analysis

Statistical analyses were performed using SPSS version 12.0 (SPSS Inc., Chicago, IL). Results were reported as mean ± standard deviation. For continuous variables, non-parametric tests (Friedman test, Wilcoxon's signed r rank test, and Mann–Whitney U test) were used. For categorical data, chi-squared test or Fisher's exact test was used. Prognostic factor analyses were performed using the Cox proportional hazards regression model. The Kaplan–Meier method was used for calculation of survival rates, and survival curves were compared by log-rank test. Multivariate analyses of factors related to enlargement of the non-irradiated region at 3 months after CIRT were performed using logistic regression analyses. Statistical significance was considered if $P < 0.05$ (P-values from two-sided tests), but for multiple comparisons of liver volume, Bonferroni's inequality was used.

Table 3
Changes in liver volume.

	Before	3 months after	6 months after	12 months after
Total (n = 43)				
Irradiated region (cm^3)	756.6 ± 134.1	696.1 ± 229.1	632.9 ± 164.2	575.9 ± 145.7
Volume variation (cm^3) (%)	−60.5 ± 204.3 (−7.8 ± 28.1)	−123.7 ± 145.7 (−15.9 ± 19.0)	−180.7 ± 104.2 (−24.0 ± 13.7)	
Non-irradiated region (cm^3)	320.0 ± 166.3	379.4 ± 169.4	389.5 ± 177.5	390.4 ± 185.7
Volume variation (cm^3) (%)	59.4 ± 80.4 (25.3 ± 37.2)	69.5 ± 85.3 (28.7 ± 36.6)	70.4 ± 85.2 (27.0 ± 33.9)	
Larger enlargement group (n = 20)				
Irradiated region (cm^3)	767.1 ± 138.1	726.7 ± 294.5	662.8 ± 178.8	582.7 ± 149.3
Volume variation (cm^3) (%)	−40.4 ± 279.8 (−4.7 ± 39.1)	−104.3 ± 177.7 (−12.7 ± 23.8)	−184.4 ± 111.9 (−24.1 ± 15.3)	
Non-irradiated region (cm^3)	317.2 ± 152.7	438.1 ± 152.0	444.9 ± 165.0	441.9 ± 162.7
Volume variation (cm^3) (%)	120.9 ± 74.1 (47.7 ± 42.6)	127.7 ± 84.0 (50.3 ± 40.5)		
Smaller enlargement group (n = 23)				
Irradiated region (cm^3)	747.5 ± 132.9	669.4 ± 154.1	606.9 ± 149.4	570.0 ± 145.7
Volume variation (cm^3) (%)	−78.1 ± 106.6 (−10.4 ± 13.2)	−140.6 ± 112.3 (−18.7 ± 13.6)	−177.5 ± 99.4 (−24.0 ± 12.4)	
Non-irradiated region (cm^3)	322.4 ± 180.6	328.3 ± 170.2	341.3 ± 177.3	345.6 ± 196.1
Volume variation (cm^3)(%)	5.9 ± 34.0 (5.8 ± 15.2)	18.9 ± 45.2 (10.0 ± 18.8)	23.2 ± 60.1 (9.6 ± 20.6)	

Values are given as mean ± standard deviation.

Results

The changes with time in liver volume values are shown in Table 3. In all patients, the volume of the irradiated region decreased significantly and that of the non-irradiated region increased significantly by the Friedman test ($P < 0.001$, $P < 0.001$, respectively), with the difference over time in the irradiated region by multiple comparisons showing that significant differences existed between any two time-points ($P < 0.001$, each). In the non-irradiated region, comparisons showed that significant differences existed between before treatment and 3, 6, and 12 months after treatment ($P < 0.001$, $P < 0.001$, $P < 0.001$, respectively), but there were no significant differences between 3 and 6 months, 3 and 12 months, and 6 and 12 months ($P = 0.091$, $P = 0.084$, and $P = 0.599$, respectively). Comparing the time-related changes of the liver volume in terms of the larger and smaller enlargement groups, both of the two groups showed significant atrophy of the irradiated region ($P < 0.001$, $P < 0.001$, respectively) and significant enlargement of the non-irradiated region ($P < 0.001$, $P = 0.022$, respectively) (Fig. 1). Further, the enlarged volume of the non-irradiated region 3 months after CIRT $\geqslant 50$ cm^3 was a prognostic factor (Table 4).

There were significant differences between the larger and smaller enlargement groups in overall survival rate and disease-free survival rate ($P = 0.030$, $P = 0.008$, respectively). Overall survival rates after 3 and 5 years were 80.0% (95% confidence interval [CI], 63–98) and 48.9% (95% CI, 27–71) in the larger enlargement group and 52.2% (95% CI, 32–73) and 29.4% (95% CI, 10–48) in the smaller enlargement group (Fig. 2a). Disease-free survival rates after 3 and 5 years were 50.0% (95% CI, 28–72) and 28.0% (95% CI, 7–49) in the larger enlargement group and 26.1% (95% CI, 8–44) and 0.0% (95% CI, 0–0) in the smaller enlargement group (Fig. 2b).

Table 5 shows the comparison of liver function between the two groups. Before treatment, there were no significant differences in serum albumin, prothrombin activity, and total bilirubin level between the two groups ($P = 0.659$, $P = 0.670$, and $P = 0.072$, respectively). Yet, 12 months after the treatment the larger enlargement group exhibited significantly higher serum albumin and prothrombin activity and lower total bilirubin levels than the smaller enlargement group ($P = 0.015$, $P = 0.002$, $P = 0.042$, respectively). As for platelet count, there were significant differences between the two groups before and after the treatment ($P = 0.002$, $P = 0.002$, respectively).

Univariate analysis showed that the planning target volume (PTV) and platelet count were significant factors for compensatory liver enlargement. Multivariate analysis showed only platelet count to be a significant factor (Table 6).

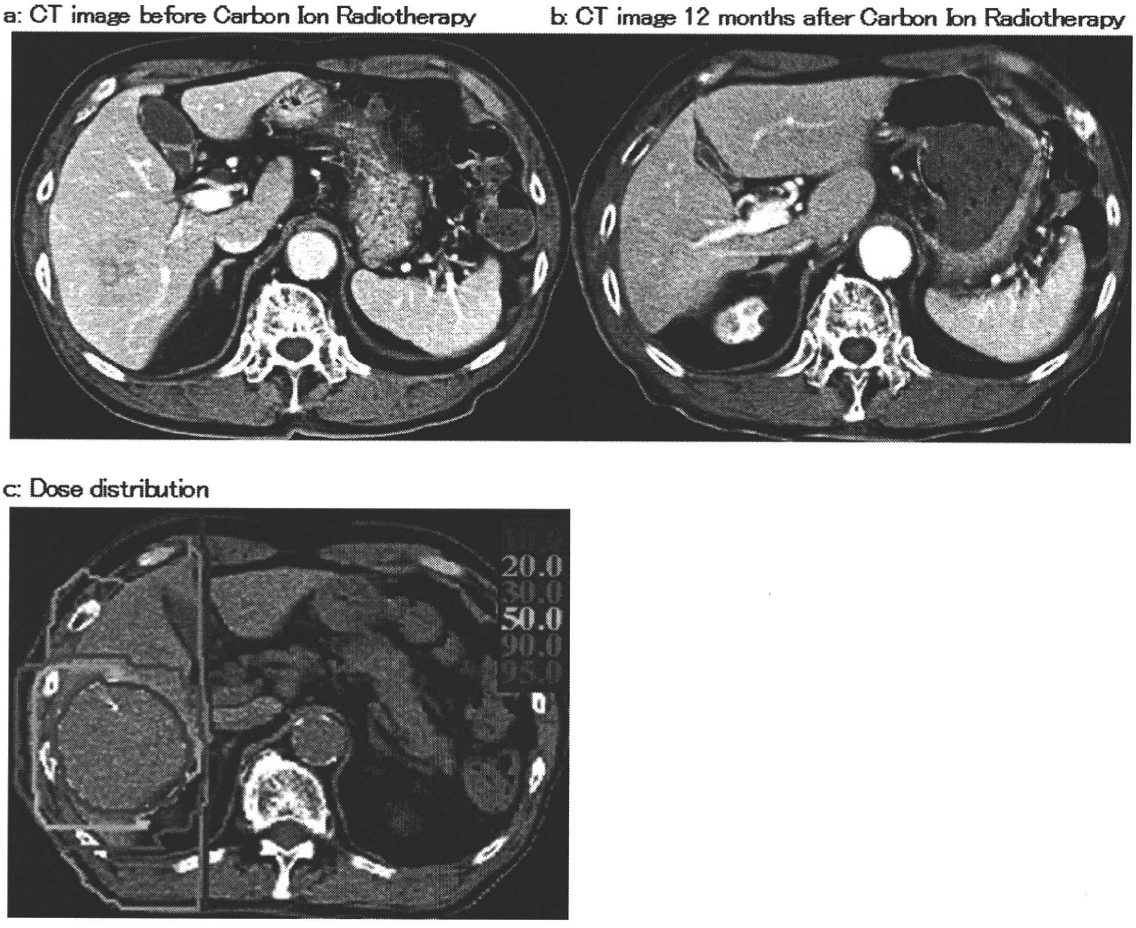

Fig. 1. CT images before and 12 months after carbon ion radiotherapy and dose distribution. CT image obtained in 81-year-old man from the larger enlargement group shows shrinkage of right hepatic lobe (840.5 cm^3 → 739.0 cm^3) and enlargement of left lateral segment (154.5 cm^3 → 266.4 cm^3). Hepatic function of this patient was retained. Serum albumin level before and 12 months after therapy was 4.5 and 4.0 g/dl, respectively. Prothrombin activity was 85.7% and 82.7%, respectively. Total bilirubin level was 0.7 and 0.7 mg/dl, respectively. Platelet count was 13.5×10^4 and $17.8 \times 10^4/\mu l$, respectively.

Table 4
Factors related to overall survival.

Factor	No. of patients	Univariate		Multivariate	
		Hazard ratio (95% CI)	*P*	Hazard ratio (95% CI)	*P*
Gender					
Male	29	1.00 (0.47–2.10)	0.994	0.55 (0.18–1.72)	0.305
Female	14				
Age (years)					
<65	15	1.12 (0.59–2.43)	0.614	1.82 (0.80–4.18)	0.155
⩾65	28				
Child-Pugh classification					
A	35	1.40 (0.63–3.10)	0.406	1.48 (0.45–4.85)	0.520
B	8				
Platelet count ($\times 10^4/\mu l$)					
<10	17	0.57 (0.29–1.15)	0.114	0.51 (0.20–1.33)	0.169
⩾10	26				
Enlargement volume of non-irradiated region at 3 months after CIRT (cm^3)					
<50	23	0.45 (0.22–0.94)	0.034	0.36 (0.15–0.88)	0.025
⩾50	20				
Planning target volume (cm^3)					
<200	24	0.78 (0.39–1.56)	0.489	1.51 (0.63–3.59)	0.357
⩾200	19				
Biological effective dose ($\alpha/\beta = 10$)					
Low (65.8–95.0)	19	0.81 (0.41–1.62)	0.555	0.95 (0.41–2.20)	0.912
High (102.3–122.5)	24				
Number of tumors					
1	36	1.07 (0.44–2.61)	0.881	0.50 (0.16–1.54)	0.226
2	7				

Discussion

In the present study, we have shown that cases with irradiation of the right lobe of the liver develop enlargement of the left lateral segment by way of compensation after CIRT and that the compensatory enlargement is contributory to the improvement of prognosis.

Approximately 80% of all HCC patients have chronic liver disorders [3], which require effective and necessarily minimally invasive therapy of HCC. We have reported that CIRT appears safe and effective for patients with HCC [22,23]. However, the reason why liver function is retained despite atrophy of the irradiated region of the liver still remained to be investigated. Hemming et al. reported that preoperative portal vein embolization performed in extended hepatectomy cases caused enlargement of the remnant liver [28]. In other research studies, enlargement of the remnant liver has been shown to have the effect of improving liver function [32–34]. Moreover, after radiotherapy, veno-occlusive diseases of the liver occur, which, it is argued, are the cause of radiation-induced liver disease [35–37]. From the above, we wonder whether the same mechanism might hold true for CIRT.

In this study, we measured the volumes of the irradiated and non-irradiated regions using CT imaging. Heymsfield and associates first measured the volume of a cadaver's liver using CT in 1979, showing that the discrepancy between the volume measured by CT and that measured using the water replacement method was

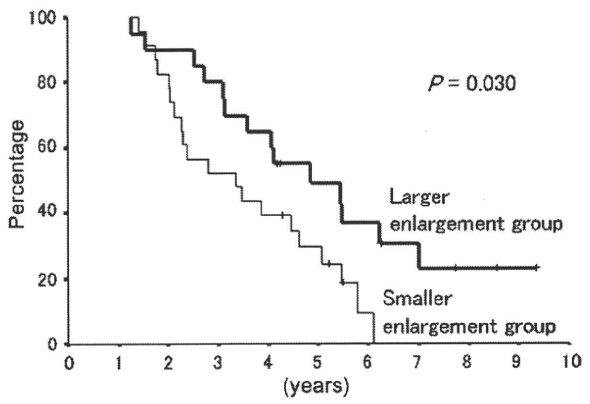

Fig. 2a. Survival rates of the larger and smaller enlargement groups. (a) Overall survival of the larger and smaller enlargement groups. Overall survival rates after 3 and 5 years were 80.0% (95% confidence interval [CI], 63–98) and 48.9% (95% CI, 27–71) in the larger enlargement group and 52.2% (95% CI, 32–73) and 29.4% (95% CI, 10–48) in the smaller enlargement group.

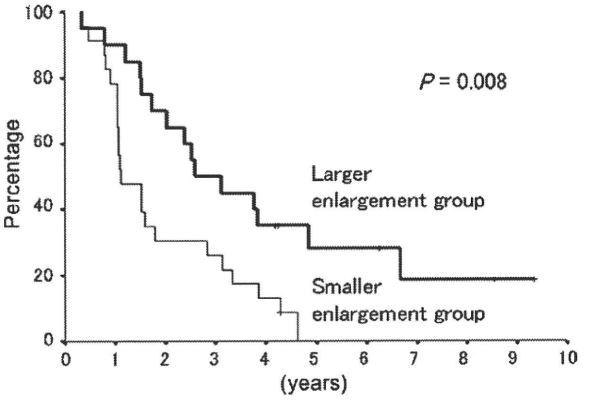

Fig. 2b. Survival rates of the larger and smaller enlargement groups. (b) Disease-free survival of the larger and smaller enlargement groups. Disease-free survival rates after 3 and 5 years were 50.0% (95% CI, 28–72) and 28.0% (95% CI, 7–49) in the larger enlargement group and 26.1% (95% CI, 8–44) and 0.0% (95% CI, 0–0) in the smaller enlargement group.

Table 5
Comparison of liver function.

	Before			12 months after		
	Larger enlargement group ($n = 20$)	Smaller enlargement group ($n = 23$)	P	Larger enlargement group ($n = 20$)	Smaller enlargement group ($n = 23$)	P
Albumin (g/dl)	3.9 ± 0.4	3.8 ± 0.4	0.659	3.9 ± 0.3	3.7 ± 0.4	0.015
Prothrombin activity (%)	78.6 ± 11.4	76.0 ± 15.3	0.670	81.9 ± 9.3	69.7 ± 11.9	0.002
Total bilirubin (mg/dl)	0.9 ± 0.3	1.1 ± 0.4	0.072	0.9 ± 0.5	1.1 ± 0.4	0.042
Platelet count ($\times 10^4$/μl)	14.0 ± 4.3	9.9 ± 3.9	0.002	14.6 ± 7.9	8.5 ± 3.4	0.002

Values are given as mean ± standard deviation.

Table 6
Factors related to compensatory enlargement.

Factor	No. of patients	Univariate P	Multivariate P	Hazard ratio	95% Confidence interval
Planning target volume (PTV) (cm^3)					
<200	24	0.013	0.147	2.92	0.69–12.46
⩾200	19				
Platelet count ($\times 10^4/\mu l$)					
<10	17	0.004	0.028	5.85	1.21–28.31
⩾10	26				
Biological effective dose (BED) ($\alpha/\beta = 10$)					
Low (65.8–95.0)	19	0.261	0.479	1.67	0.40–6.94
High (102.3–122.5)	24				

within 5% [38]. In 1981, Moss et al. also measured liver volume using CT, confirming the conclusion of Heymsfield et al. [39]. Many studies have reported that the difference between CT-measured liver volume and the actual liver volume is minor [38–40]. In our study, the volume of the left lateral segment was 320.0 ± 166.3 cm^3 (Table 3). Zhou et al. measured the volume of 113 hepatic lobes using CT. They reported average volumes of the left lateral segment of 313.2 ± 105.1 and 282.2 ± 136.2 cm^3 in Child-Pugh class A and B patients, respectively [41]. These results generally resemble ours, lending support to the accuracy and reliability of our measuring method.

It is difficult to distinguish strictly the irradiated and non-irradiated portions, and therefore in this study we defined the left lateral segment of the liver as the non-irradiated region, and the other segments as irradiated. In 11 of 43 patients, the region considered as irradiated was larger than the region really receiving radiation. We cannot examine whether the non-irradiated portions of the right lobes enlarge or not because it is difficult to distinguish the irradiated and non-irradiated portions of the right lobe. The volumes of the irradiated part of the liver measured at 0, 3, 6, and 12 months after treatment, respectively, did show significant differences. With the lapse of time, the measurement values decreased significantly. In contrast, the liver volumes of the non-irradiated part increased at 3 months post-treatment on a significant scale compared to before the treatment. From then on, no more significant increases were observed. These data demonstrate that the enlargement of the non-irradiated region is not a matter of the natural course associated with chronic liver disorders, but rather results as compensation for the CIRT-caused atrophy of the liver.

We divided the subjects into two groups according to compensatory enlargement liver volume of more or less than 50 cm^3 because enlarged volume of the non-irradiated region 3 months after CIRT ⩾50 cm^3 was a prognostic factor. In terms of liver function, many complex methods for estimating liver functional reserve have been advocated, including tests that measure liver metabolic activity such as ICG clearance, galactose elimination, and aminopyrine clearance [42]. However, it was demonstrated that either one of Child classification [43] or Okuda staging [44] is highly predictive for outcome [45]. Serum albumin, prothrombin activity, and total bilirubin level are the serum items of the Child-Pugh score, which is the index of hepatic functional reserve. Therefore, Serial changes in these items were reviewed as hepatic functional reserve before and 12 months after treatment in the two groups. There were no significant differences in them before the treatment, but at 12 months after, the larger enlargement group remained significantly more favorable than the smaller enlargement group. On the other hand, the extent of atrophy of the irradiated regions was found to be significantly similar in the two groups. These data indicate the possibility that the compensatory enlargement, taking place in the non-irradiated region of the liver after CIRT, affect hepatic functional reserve. It was suggested that better disease-free survival and hepatic functional reserve contributed to improvement of overall survival.

We investigated PTV, platelet count, and biological effective dose (BED) as indicators of enlargement of the non-irradiated region at 3 months after CIRT. PTV and platelet count were selected on the basis of their significant differences between the larger and smaller enlargement groups. In our study, it was difficult to compare the differences of total dose and fractionations because of their various combinations. Then, although it has not been confirmed that BED is adaptable to CIRT, we tried to calculate BED for every fractionation by L/Q model [46], adding it to the variables. The difference in mean age between the two groups was thought not to be related to the compensatory enlargement of the liver after CIRT, based on the self-evident discrepancy between age and the enlargement volume, i.e., the higher the age, the larger the volume. Therefore, we excluded age from the analysis of the indicators of compensatory enlargement of the non-irradiated liver. Our data demonstrated platelet count to be the major factor of compensatory enlargement of the non-irradiated liver, and it is known that platelet count decreases in parallel with the grade of chronic liver disease [47]. Thus, we intend to investigate the relationship between liver fibrosis and compensatory enlargement of the liver in future studies.

Considering the limitations of this study, we must first point out the nature of the investigation as a retrospective one. Secondly, the subjects were restricted to cases in which target tumors were located in the right lobe of the liver. Thirdly, we did not utilize any biochemical or molecular biological method.

It was demonstrated that the non-irradiated region of the liver enlarged compensatively until 3 months after CIRT and that the enlarged volume of this region 3 months after CIRT ⩾50 cm^3 was a prognostic factor. We can conclude that compensatory enlargement of the non-irradiated liver contributes to the improvement of prognosis.

Conflict of interest statement

Any actual or potential conflicts of interest do not exist.

Acknowledgments

This study was supported by the Research Project with Heavy Ions of the National Institute of Radiological Sciences in Japan. We are grateful to members of the National Institute of Radiological Sciences. We are indebted to Dr. Gen Kobashi and Dr. Kaori Ohta for statistical support.

References

[1] Bosch FX, Ribes J, Borras J. Epidemiology of primary liver cancer. Semin Liver Dis 1999;19:271–85.
[2] Marugame T, Matsuda T, Kamo K, et al. Cancer incidence and incidence rates in Japan in 2001 based on the data from 10 population-based cancer registries. Jpn J Clin Oncol 2007;37:884–91.
[3] Ikai I, Arii S, Okazaki M, et al. Report of the 17th Nationwide Follow-up Survey of Primary Liver Cancer in Japan. Hepatol Res 2007;37:676–91.
[4] Mulcahy MF. Management of hepatocellular cancer. Curr Treat Options Oncol 2005;6:423–35.
[5] Kuvshinoff BW, Ota DM. Radiofrequency ablation of liver tumors: influence of technique and tumor size. Surgery 2002;132:605–11.
[6] Shiina S, Teratani T, Obi S, et al. A randomized controlled trial of radiofrequency ablation with ethanol injection for small hepatocellular carcinoma. Gastroenterology 2005;129:122–30.
[7] Sato M, Watanabe Y, Ueda S, et al. Microwave coagulation therapy for hepatocellular carcinoma. Gastroenterology 1996;110:1507–14.
[8] Camma C, Schepis F, Orlando A, et al. Transarterial chemoembolization for unresectable hepatocellular carcinoma: meta-analysis of randomized controlled trials. Radiology 2002;224:47–54.
[9] Lo CM, Ngan H, Tso WK, et al. Randomized controlled trial of transarterial lipiodol chemoembolization for unresectable hepatocellular carcinoma. Hepatology 2002;35:1164–71.
[10] Llovet JM, Real MI, Montana X, et al. Arterial embolization or chemoembolization versus symptomatic treatment in patients with unresectable hepatocellular carcinoma: a randomized controlled trial. Lancet 2002;359:1734–9.
[11] Higuchi T, Kikuchi M, Okazaki M. Hepatocellular carcinoma after transcatheter hepatic arterial embolization. A histopathologic study of 84 resected cases. Cancer 1994;73:2259–67.
[12] Adachi E, Matsumata T, Nishizaki T, Hashimoto H, Tsuneyoshi M, Sugimachi K. Effects of preoperative transcatheter hepatic arterial chemoembolization for hepatocellular carcinoma. The relationship between postoperative course and tumor necrosis. Cancer 1993;72:3593–8.
[13] Phillips R, Murikami K. Preliminary neoplasms of the liver. Results of radiation therapy. Cancer 1960;13:714–20.
[14] Stillwagon GB, Order SE, Guse C, et al. 194 hepatocellular cancers treated by radiation and chemotherapy combinations: toxicity and response: a Radiation Therapy Oncology Group study. Int J Radiat Oncol Biol Phys 1989;17:1223–9.
[15] Zhao JD, Xu ZY, Zhu J, et al. Application of active breathing control in 3-dimensional conformal radiation therapy for hepatocellular carcinoma: the feasibility and benefit. Radiother Oncol 2008;87:439–44.
[16] Toya R, Murakami R, Baba Y, et al. Conformal radiation therapy for portal vein tumor thrombosis of hepatocellular carcinoma. Radiother Oncol 2007;84:266–71.
[17] Robertson JM, Lawrence TS, Dworzanin LM, et al. Treatment of primary hepatobiliary cancers with conformal radiation therapy and regional chemotherapy. J Clin Oncol 1993;11:1286–93.
[18] Suit HD, Goitein M, Munzenrider J, et al. Increased efficacy of radiation therapy by use of proton beam. Strahlenther Onkol 1990;166:40–4.
[19] Matsuzaki Y, Osuga T, Saito Y, et al. A new, effective, and safe therapeutic option using proton irradiation for hepatocellular carcinoma. Gastroenterology 1994;106:1032–41.
[20] Kanai T, Endo M, Minohara S, et al. Biophysical characteristics of HIMAC clinical irradiation system for heavy-ion radiation therapy. Int J Radiat Oncol Biol Phys 1999;44:201–10.
[21] Kanai T, Furusawa Y, Fukutsu K, Itsukaichi H, Eguchi-Kasai K, Ohara H. Irradiation of mixed beam and design of spread-out Bragg peak for heavy-ion radiotherapy. Radiat Res 1997;147:78–85.
[22] Kato H, Tsujii H, Miyamoto T, et al. Results of the first prospective study of carbon ion radiotherapy for hepatocellular carcinoma with liver cirrhosis. Int J Radiat Oncol Biol Phys 2004;59:1468–76.
[23] Kato H, Yamada S, Yasuda S, et al. Phase II study of short-course carbon ion radiotherapy (52.8GyE/4-fraction/1-week) for hepatocellular carcinoma. Hepatology 2005;42(Suppl. 1):381A.
[24] Blakely EA, Ngo FQH, Curtis SB, et al. Heavy ion radiobiology: cellular studies. Adv Radiat Biol 1984;11:295–378.
[25] Castro JR. Future research strategy for heavy ion radiotherapy. In: Kogelnih HD, editor. Progress in radio-oncology. Bologna: Monduzzi Editore; 1995. p. 643–8.
[26] Tsujii H, Morita S, Miyamoto T, et al. Preliminary results of phase I/II carbon ion therapy. J Brachyther Int 1997;13:1–8.
[27] Suzuki M, Kase Y, Yamaguchi H, Kanai T, Ando K. Relative biological effectiveness for cell-killing effect on various human cell lines irradiated with heavy-ion medical accelerator in Chiba (HIMAC) carbon-ion beams. Int J Radiat Oncol Biol Phys 2000;48:241–50.
[28] Hemming AW, Reed AI, Howard RJ, et al. Preoperative portal vein embolization for extended hepatectomy. Ann Surg 2003;237:686–91.
[29] Abulkhir A, Limongelli P, Healey AJ, et al. Preoperative portal vein embolization for major liver resection: a meta-analysis. Ann Surg 2008;247:49–57.
[30] Sato K, Yamada H, Ogawa K, et al. Performance of HIMAC. Nucl Phys 1995;A588:229–34.
[31] Minohara S, Kanai T, Endo M, Noda K, Kanazawa M. Respiratory gated irradiation system for heavy-ion radiotherapy. Int J Radiat Oncol Biol Phys 2000;47:1097–103.
[32] Kubo S, Shiomi S, Tanaka H, et al. Evaluation of the effect of portal vein embolization on liver function by (99m)tc-galactosyl human serum albumin scintigraphy. J Surg Res 2002;107:113–8.
[33] Kudo M, Todo A, Ikekubo K, Yamamoto K, Vera DR, Standalnik RC. Quantitative assessment of hepatocellular function through in vivo radioreceptor imaging with technetium 99m galactosyl human serum albumin. Hepatology 1993;17:814–9.
[34] Vera DR, Topcu SJ, Stadalnik RC. In vitro quantification of asialoglycoprotein receptor density from human hepatic microsamples. Methods Enzymol 1994;247:394–402.
[35] Reed Jr GB, Cox Jr AJ. The human liver after radiation injury. A form of veno-occlusive disease. Am J Pathol 1966;48:597–611.
[36] Lawrence TS, Robertson JM, Anscher MS, Jirtle RL, Ensminger WD, Fajardo LF. Hepatic toxicity resulting from cancer treatment. Int J Radiat Oncol Biol Phys 1995;31:1237–48.
[37] Cheng JC, Wu JK, Huang CM, et al. Radiation-induced liver disease after radiotherapy for hepatocellular carcinoma: clinical manifestation and dosimetric description. Radiother Oncol 2002;63:41–5.
[38] Heymsfield SB, Fulenwider T, Nordlinger B, Barlow R, Sones P, Kutner M. Accurate measurement of liver, kidney, and spleen volume and mass by computerized axial tomography. Ann Intern Med 1979;90:185–7.
[39] Moss AA, Friedman MA, Brito AC. Determination of liver, kidney, and spleen volumes by computed tomography: an experimental study in dogs. J Comput Assist Tomogr 1981;5:12–4.
[40] Sakamoto S, Uemoto S, Uryuhara K, et al. Graft size assessment and analysis of donors for living donor liver transplantation using right lobe. Transplantation 2001;71:1407–13.
[41] Zhou XP, Lu T, Wei YG, Chen XZ. Liver volume variation in patients with virus-induced cirrhosis: findings on MDCT. AJR Am J Roentgenol 2007;189:W153–159.
[42] Friedman LS, Martin P, Santiago JM. Liver function tests and the objective evaluation of the patient with liver disease. In: Zakim D, Boyer TD, editors. Hepatology. Philadelphia: WB Saunders; 1996. p. 791–833.
[43] Wants GE, Payne MA. Experience with portacaval shunt for portal hypertension. N Engl J Med 1961;265:721–8.
[44] Okuda K, Ohtsuki T, Obata H, et al. Natural history of hepatocellular carcinoma and prognosis in relation to treatment. Cancer 1985;56:918–28.
[45] Fong Y, Sun RL, Jarnagin W, et al. An analysis of 412 cases of hepatocellular carcinoma at a western center. Ann Surg 1999;229:790–9.
[46] Lee SP, Leu MY, Smathers JB, et al. Biologically effective dose distribution based on the linear quadratic model and its clinical relevance. Int J Radiat Oncol Biol Phys 1995;33:375–89.
[47] Karasu Z, Tekin F, Ersoz G, et al. Liver fibrosis is associated with decreased peripheral count in patients with chronic hepatitis B and C. Dig Dis Sci 2007;52:1535–9.

Journal of Gastroenterology and Hepatology

JGHF

doi:10.1111/j.1440-1746.2010.06248.x

HEPATOLOGY

Carbon dioxide-based portography: An alternative to conventional imaging with the use of iodinated contrast medium

Hitoshi Maruyama, Hidehiro Okugawa, Hiroyuki Ishibashi, Masanori Takahashi, Satoshi Kobayashi, Hiroaki Yoshizumi and Osamu Yokosuka

Department of Medicine and Clinical Oncology, Chiba University Graduate School of Medicine, Chiba, Japan

Key words
carbon dioxide, contrast medium, portography, portal hypertension.

Accepted for publication 20 December 2009.

Correspondence
Hitoshi Maruyama, Department of Medicine and Clinical Oncology, Chiba University Graduate School of Medicine, 1-8-1, Inohana, Chuou-ku, Chiba, 260-8670, Japan. Email: maru-cib@umin.ac.jp

Abstract

Background and Aim: To clarify the efficacy of carbon dioxide (CO_2) as a contrast material to evaluate portal vein images by percutaneous transhepatic portography (PTP).

Methods: Twenty patients (38–76 years; male 13, female 7) with chronic liver diseases were the subjects of this prospective study. Portal venous opacification by PTP was compared between CO_2-based images and iodinated contrast medium (ICM)-based images by two independent reviewers, according to the three-grade scoring; 0 for none, 1 for weak and 2 for sufficient.

Results: Total scores of extrahepatic portal veins (137 for CO_2, 93 for ICM), collateral vessels (64 for CO_2, 60 for ICM) and intrahepatic portal veins (69 for CO_2, 76 for ICM) were not statistically significant between CO_2-based and ICM-based images ($P = 0.0623$). Sufficient opacification of superior mesenteric vein was more frequent on CO_2-based images (none 0, weak 4, sufficient 16) than ICM-based images (none 19, weak 0, sufficient 1; $P < 0.0001$). The score was not statistically significant between CO_2-based and ICM-based images in portal trunk, splenic vein, inferior mesenteric vein and other collateral vessels. Although opacification grade in the intrahepatic left portal vein was not statistically significant between CO_2-based and ICM-based images ($P = 0.1515$), weak opacification was significantly frequent on CO_2-based images (weak 10, sufficient 10) compared to ICM-based images (weak 0, sufficient 20; $P = 0.0003$) in the intrahepatic right portal vein. Inter-reviewer agreement was excellent between the two reviewers for CO_2-based images (kappa = 0.913) and ICM-based images (kappa = 0.924).

Conclusions: Carbon dioxide may be a first-line contrast material for evaluating portal vein images by PTP.

Introduction

Because of the development of high-performance medical accessories, interventional radiology has gained wide popularity and extended application. As a consequence, iodinated contrast medium (ICM) has been frequently used via intravascular injection for diagnosis and treatment procedures in clinical practice. However, as ICM sometimes causes severe adverse events such as renal toxicity and/or allergy, reduction in the frequency of ICM use is now occurring worldwide.[1,2]

Carbon dioxide (CO_2) is recognized as an effective contrast material for vascular enhancement during angiography, because of its safety, low viscosity, stable effect and low cost, based on a prevalence of the digital subtraction angiography (DSA) system.[3,4] Previous studies have shown the clinical utility of splenoportography and wedge hepatic venography with the use of CO_2 to present portal vein images.[5–8] However, these methods have some limitations, as they do not allow the treatment of embolization for collateral vessels or dilation for stenotic vessels. Furthermore, they have the disadvantage of being unable to measure portal pressure, as it is not provided by splenoportography and nor, in the case of pre-sinusoidal obstruction, by wedge hepatic venography.[9]

Percutaneous transhepatic portography (PTP) is a well-established angiographic technique that provides a detailed portal venous appearance and measurement of portal venous pressure.[10–12] Although its invasive aspect may be a shortcoming, PTP still remains an essential procedure especially in treatment-required cases.[5,13,14] However, the efficacy of the use of CO_2 to evaluate the portal venous appearance during the PTP process has not been fully discussed.

Based on these backgrounds, we have designed this prospective study to compare the grade of opacification of each of the portal veins and collateral vessels between CO_2-based and ICM-based portograms. The aim of this study was to clarify the efficacy of

CO_2 as a contrast material to evaluate portal vein images as an alternative to ICM during the PTP procedure.

Methods

Patients

Between February 2007 and August 2009, a prospective study was performed at the Chiba University Hospital, Chiba, Japan, after the approval of the ethics committee, with informed written consent from all patients. Inclusion criteria were: (i) cirrhosis or idiopathic portal hypertension (IPH) patients just after effective treatment of esophageal varices by endoscopic sclerotherapy; (ii) cirrhosis or IPH patients scheduled to undergo radiological treatment of gastric fundal varices diagnosed by endoscopy; and (iii) patients with scheduled PTP to examine portal hemodynamics informative for subsequent clinical management. Exclusion criteria were: (i) patients with liver dysfunction of Child–Pugh C grade not being candidates for variceal treatment; (ii) patients with ascites, portal vein thrombosis or focal hepatic lesion on sonogram; (iii) patients with severe impaired coagulation, platelet count less than 50 000/μL or prothrombin time less than 40%.

The subjects were 20 consecutive patients (age: 38–76 years, 59 ± 11; male 13, female 7), 16 with cirrhosis (age: 38–76 years, 59 ± 11; male 10, female 6) and 4 with IPH (age: 49–69, 59 ± 10; male 3, female 1). Thirteen patients had esophageal varices that were effectively treated and seven patients had gastric fundal varices deserving to be treated (elective treatment in 5, prophylactic treatment in 2). At the time of PTP, patients with suspected IPH or with negative findings of hepatitis B or C virus infection received concomitant hepatic venography. Free and wedged hepatic venous pressures were measured to examine for the presence of the pathophysiology of pre-sinusoidal block, which is a characteristic finding in IPH. Histological diagnosis of the liver was made in all 20 patients by liver biopsy after PTP: non-cirrhotic specimens in 4, cirrhosis in 16 with etiology of hepatitis C virus in 6, alcohol abuse in 4, autoimmune in 3, hepatitis B virus in 1, non-alcoholic steatohepatitis in 2. In the cirrhosis patients, the degree of liver function reserve as classified by Child-Pugh scoring system was A in 10 and B in 6. Diagnosis of IPH for the remaining 4 patients was based on blood tests, hepatic venography and histology from biopsy specimens in all patients according to the general rules for the study of portal hypertension.[15]

Percutaneous transhepatic portography

The angio machine used in this study was Infinix Celeve-VB110A/J1 (Toshiba, Tokyo, Japan) with the standard DSA system. Portal vein catheterization was performed by means of an ultrasound-guided procedure with regional anesthesia and intravenous sedation in the supine position. Then, a 4-Fr catheter (SV-2, Hanako Medical, Saitama, Japan) was advanced to the splenic hilum by plastic-coated guidewire (Radifocus guidewire M, 0.035; Terumo, Tokyo, Japan). The settings of the angio machine were 82 kV, 630 mA, 38.00 ms and 5.0 f/s for CO_2 injection, and 82 kV, 400 mA, 55.00 ms and 3.0 f/s for ICM injection. As for the CO_2 injection, a 50-cc syringe was connected to the tank via three-way stopcock, and 40 cc of CO_2 was prepared in the syringe. Care was taken to close the tip of the syringe with the stopcock after filling of CO_2 to avoid air contamination.[16] Portograms were taken twice, firstly by CO_2 injection manually and rapidly, and secondly by ICM injection (30 mL, 5 mL/s, Omnipaque300, Daiichi-Sankyo, Tokyo, Japan) by means of a mechanical injection system (Mark V ProVis, MEDRAD, Warrendale, PA, USA). The approximate time of fluoroscopy was 5 s for CO_2 based-images and 10 s for ICM-based images from the beginning of the contrast material injection. All PTP procedures were performed by HO, HI and MT, hepatologists and radiologists with more than 7 years of experience at the time of the initial case. Complications were assessed by clinical symptoms and monitoring of vital signs including blood pressure, pulse rate, oxygen saturation, electrocardiogram and urine volume during and after the examinations. Furthermore, ultrasound observations and blood tests were added on the following day to check for adverse events; the former for ascites due to intraperitoneal bleeding from the liver surface, intrahepatic arterioportal communication resulting from the puncture, and portal vein thrombosis due to the catheterization, and the latter for liver and renal dysfunction, and anemia.

Review process of portograms

Four representative photograms of approximately maximum opacification in the intra-, and extrahepatic portal veins and collateral vessels were selected from each cine image of CO_2-based and ICM-based portograms by HM, a hepatologist and radiologist with more than 17 years of experience at the time of the initial case. These eight photograms, four CO_2-based images and four ICM-based images, were printed out and forwarded to the review process. The review was conducted for the following vessels: intrahepatic right and left portal veins, extrahepatic portal veins including portal trunk, splenic vein, superior mesenteric vein and inferior mesenteric vein, and collateral vessels including left gastric vein, posterior gastric vein, short gastric vein, and paraumbilical vein. The review criteria for portal vein findings were based on the scoring of three grades of opacification: 0 for none, 1 for weak, and 2 for sufficient.

There were two independent reviewers in our study, A (SK) and B (HY), hepatologists and radiologists with more than 9 years of experience at the time of the initial case. The review results for the opacification grade in the vessels were compared between CO_2-based images and ICM-based images. Consensual decision-making by the two reviewers was applied to lack-of-consensus review results to obtain the final score.

Statistical analysis

The Chi-square test was used for comparison of the total scores reviewed for intrahepatic portal veins, extrahepatic portal veins and collateral vessels between CO_2-based and ICM-based images, and for comparison of the differences in the grade of opacification in each vessel between ICM-based and CO_2-based images. Inter-reviewer (reviewer A *vs* B) agreement was assessed by Kappa value calculation. Agreement grade was defined as < 0.2 for poor, 0.2–0.4 for moderate, 0.4–0.6 for fair, 0.6–0.8 for good, and 0.8–1.0 for excellent. Statistical significance was taken

at $P < 0.05$. Statistical analysis was performed using the Dr SPSS package (version 11.0J for Windows; SPSS Inc., Chicago, IL, USA).

Results

Comparison of portograms between CO_2-based images and ICM-based images

CO_2- and ICM-based portograms were successfully obtained in all subjects without any adverse events during and after PTP examinations (Figs. 1,2). Total scores reviewed in the extrahepatic portal veins (137 for CO_2, 93 for ICM), collateral vessels (64 for CO_2, 60 for ICM) and intrahepatic portal veins (69 for CO_2, 76 for ICM) were not statistically significant between CO_2-based and ICM-based images ($P = 0.0623$, Table 1). Inter-reviewer agreement was excellent between reviewers A and B for CO_2-based images (kappa = 0.913) and ICM-based images (kappa = 0.924).

Difference in opacification grade in each of the portal veins between CO_2-based images and ICM-based images

In the extrahepatic portal veins, the scores in the portal trunk and splenic vein were identical between CO_2-based and ICM-based images, and the scores in the inferior mesenteric vein were not statistically significant between them ($P = 0.1626$, Table 1). However, sufficient opacification of the superior mesenteric vein was more frequent on CO_2-based images (none 0, weak 4, sufficient 16) than ICM-based images (none 19, weak 0, sufficient 1; $P < 0.0001$). As for the collateral vessels, the scores in the paraumbilical vein were identical between CO_2-based and ICM-based images. In addition, the scores were not statistically significant between CO_2-based and ICM-based images in the left gastric vein ($P = 0.1889$), posterior gastric vein ($P = 0.5244$), and short gastric vein ($P = 0.6298$).

Although the opacification grade in the intrahepatic left portal vein was not statistically significant between CO_2-based images (weak 1, sufficient 19) and ICM-based images (weak 4, sufficient 16; $P = 0.1515$), weak opacification was significantly frequent on CO_2-based images (weak 10, sufficient 10) compared to ICM-based images (weak 0, sufficient 20, $P = 0.0003$) in the intrahepatic right portal vein.

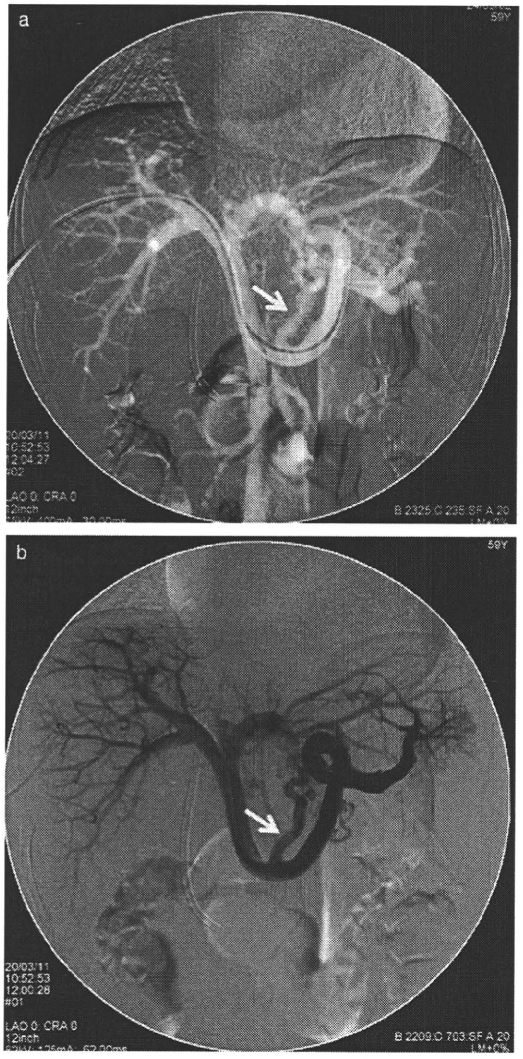

Figure 1 59-year old female, cirrhosis caused by autoimmune hepatitis, after treatment of esophageal varices. (a) CO_2-based portogram. Portal trunk, splenic vein, superior mesenteric vein, left gastric vein (arrow), and intrahepatic portal veins were sufficiently opacified. (b) ICM-based portogram. Portal trunk, splenic vein, left gastric vein (arrow), and intrahepatic portal veins were sufficiently opacified. However, superior mesenteric vein was not demonstrated on this image. CO_2, carbon dioxide; ICM, iodinated contrast medium.

Discussion

Offering technical improvement with a reduction in the incidence of adverse events is an obvious benefit for patients. Our study proved the efficacy of CO_2 as a contrast material for the evaluation of portal venous appearance during PTP examination, with the non-requirement of a mechanical power injector. CO_2-based PTP may become a standard and reliable procedure for the detailed examination of portal hemodynamics in patients with portal hypertension.

Carbon dioxide has the beneficial aspects of an intravascular rapid diffusion property as well as non-toxicity.[3,4] This diffusion factor may be the reason for the better demonstration of the superior mesenteric vein on CO_2-based images than ICM-based images, although this vessel has hepatopetal flow direction against the spreading of contrast material discharged from the splenic hilum to opacify the vessel. It should be emphasized that CO_2 allows wider visualization of the extrahepatic portal venous system under shorter fluoroscopy time than ICM, and this advantage may substantially reduce radiation exposure. However, it remains to be elucidated if CO_2 discharged from the superior mesenteric vein may provide sufficient demonstration of the splenic vein and the other collateral vessels derived from the splenic vein.

Contrast material was injected in a single uniform way in our study—30 mL of ICM and 40 cc of CO_2. The former is a standard

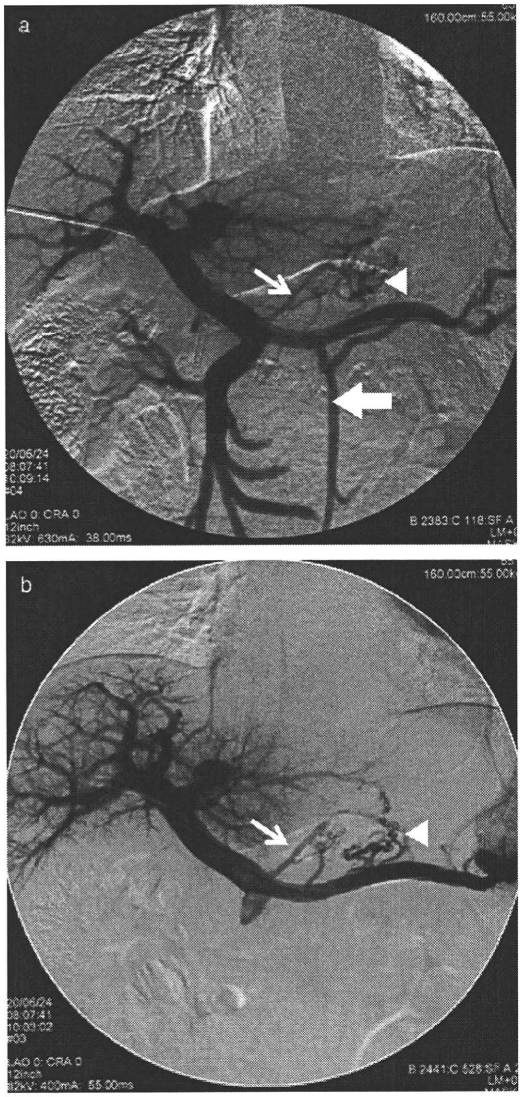

Figure 2 65-year old male, cirrhosis caused by non-alcoholic steatohepatitis, after treatment of esophageal varices. (a) CO_2-based portogram. Portal trunk, splenic vein, superior mesenteric vein, left gastric vein (arrow), posterior gastric vein (arrow head), inferior mesenteric vein (thick arrow), and intrahepatic left portal vein were sufficiently opacified. However, intrahepatic right portal vein had weak opacification on this image. (b) ICM-based portogram. Portal trunk, splenic vein, left gastric vein (arrow), posterior gastric vein (arrow head), and intrahepatic portal veins were sufficiently opacified. However, neither superior mesenteric vein nor inferior mesenteric vein was demonstrated on this image. CO_2, carbon dioxide; ICM, iodinated contrast medium.

dose in our department and in the literature,[17] and the latter was defined based on previous reports: 30–40 cc of CO_2 was given to adults in the study by Caridi *et al.*[6] and the safety of 80 cc of CO_2 for average-size patients was reported by Hawkins *et al.*[4] In addition, an actual, reasonable aspect was that the commonly available largest syringe was 50 cc in size, and the approximately 80%-filled 50-cc syringe presented an easy-handling manner for manual injection. In fact, as there were no adverse events from CO_2 injection in our study, the safety of 40 cc of CO_2 for adults was also proven. However, as the injection of a large volume of CO_2 causes displacement of blood from the right side of the heart, a serious complication called 'vapor lock', operators should be careful about the excessive use of CO_2.[4] As for the injection of CO_2, additionally, contamination with air should also be strictly avoided, especially in patients with portal hypertension, as they have portosystemic collateral vessels on one level or another. It is reported that most of the patients with gastric fundal varices had a large gastrorenal shunt, a major outflow route of varices into the inferior vena cava via the left renal vein.[18] Obviously, unnecessary injection of CO_2 should be avoided, and the volume of CO_2 might preferably be prepared based on conditions such as body mass index (BMI) of the subject and/or the vessels to be opacified.

Thanks to the development of digital technologies, non-invasive assessment with the use of ultrasound or magnetic resonance imaging (MRI) has been available for portal hemodynamics, while clinical interests of direct catheterization into the portal vein might have dropped off.[19,20] However, in spite of their benefits, these apparently convenient modalities also seem to have some disadvantages. Taourel *et al.* reported that portal velocity or flow on Doppler measurement had limited utility in predicting either hepatic venous pressure gradients or severity of liver failure in an individual patient because of the scattering of the data.[21] According to the study by Lin *et al.* three-dimensional contrast-enhanced MR portography had a limitation in the differential diagnosis of portal vein between narrowing and obstruction, although it had the advantage of detecting a small thrombus in the portal vein.[22] In addition, results obtained by ultrasound observation depend on the patient's body habitus and the operator's skill, and the generally insufficient prevalence of MRI equipment is still a problem for its widespread application. The PTP technique is directly effective for the treatment of dilatation or obstruction of impaired portal vein.[13,23–26] The use of PTP with CO_2 may continue to play an important role in the clinical management of patients with portal hypertension in spite of the invasiveness.

There were some limitations to our study. First, weak opacification in the intrahepatic right portal vein was more frequent on CO_2-based images than ICM-based images, a propensity not found in the intrahepatic left portal vein. The authors speculated that gravity might have forced CO_2 to the left portal vein branch in the supine-positioned patient because of its high buoyancy.[4] In addition, as the intrahepatic right portal vein is the farthest vessel from the catheter tip at the splenic hilum, it is open to a variety of influences of CO_2 distribution after the discharge. In any event, the CO_2-based portogram may underestimate the findings of intrahepatic right portal vein branches, though this might be resolved by changing the position of the body, placement of the catheter tip, or CO_2 volume. However, as the effects of these additional techniques have not been investigated, underestimation of intrahepatic right portal vein should be realized as a disadvantage of CO_2-based portography. Second, opacification of collateral vessels was assessed after the completion of variceal treatment in patients with esophageal varices, because evaluation of portal hemodynamics by PTP after the treatment was considered beneficial for the subsequent management of the patients.[27]

Table 1 Comparison of the grade of opacification in the portal vein between CO_2-based images and ICM-based images

	PT	SV	SMV	IMV	LGV	PGV	SGV	PUV	RPV	LPV
CO_2, A	0/0/20	0/0/20	0/4/16	7/5/8	5/7/8	9/6/5	7/10/3	17/0/3	0/10/10	0/1/19
CO_2, B	0/0/20	0/0/20	0/5/15	7/5/8	4/6/10	9/6/5	7/8/5	17/0/3	0/9/11	0/1/19
CO_2, F	0/0/20	0/0/20	0/4/16	7/5/8	4/6/10	9/6/5	7/10/3	17/0/3	0/10/10	0/1/19
	(40)	(40)	(36)	(21)	(26)	(16)	(16)	(6)	(30)	(39)
ICM, A	0/0/20	0/0/20	19/1/0	13/3/4	8/2/10	11/3/6	5/11/4	17/0/3	0/0/20	0/4/16
ICM, B	0/0/20	0/0/20	19/0/1	13/4/3	9/1/10	11/3/6	5/13/2	17/0/3	0/0/20	0/7/13
ICM, F	0/0/20	0/0/20	19/0/1	13/3/4	8/2/10	11/3/6	5/13/2	17/0/3	0/0/20	0/4/16
	(40)	(40)	(2)	(11)	(22)	(15)	(17)	(6)	(40)	(36)

Extrahepatic portal veins:
IMV, inferior mesenteric vein; PT, portal trunk; SMV, superior mesenteric vein; SV, splenic vein.
Collateral vessels:
LGV, left gastric vein; PGV, posterior gastric vein; PUV, paraumbilical vein; SGV, short gastric vein.
Intrahepatic portal veins:
LPV, intrahepatic left portal vein; RPV, intrahepatic right portal vein.
CO_2, carbon dioxide; ICM, iodinated contrast medium.
Number, none/weak/sufficient, grade of opacification reviewed by the reviewer.
Number shown in parentheses, scoring by 0 for none, 1 for weak and 2 for sufficient.
A, reviewer A; B, reviewer B; F, final review result.

Therefore, the left gastric vein, a major inflow route for esophageal varices, was in a treatment-modified status in the present study, and the effectiveness of CO_2 in demonstrating the treatment-unmodified left gastric vein, in a narrow sense, has still to be elucidated.

In conclusion, although additional study with large numbers of patients would be required to confirm our results, CO_2 may be a first-line contrast material for evaluating portal vein images by PTP, except for the visualization of intrahepatic right portal vein. The specific utility of CO_2-based portography in clinical practice still needs to be thoroughly investigated.

References

1 Waybill MM, Waybill PN. Contrast media-induced nephrotoxicity: identification of patients at risk and algorithms for prevention. *J. Vasc. Interv. Radiol.* 2001; **12**: 3–9.
2 Mehran R, Nikolsky E. Contrast-induced nephropathy: definition, epidemiology and patients at risk. *Kidney Int.* 2006; **Apr** (Suppl 100): S11–15.
3 Kerns SR, Hawkins IF. Carbon dioxide digital subtraction angiography: expanding applications and technical evolution. *AJR Am. J. Roentgenol.* 1995; **164**: 735–41.
4 Hawkins IF, Caridi JG. Carbon dioxide (CO_2) digital subtraction angiography: 26-year experience at the University of Florida. *Eur. Radiol.* 1998; **8**: 391–402.
5 Burke CT, Weeks SM, Mauro MA, Jaques PF. CO_2 Splenoportography for evaluating the splenic and portal veins before and after liver transplantation. *J. Vasc. Interv. Radiol.* 2004; **15**: 1161–5.
6 Caridi JG, Hawkins Jr. IF, Cho K *et al.* CO_2 Splenoportography: preliminary results. *AJR Am. J. Roentgenol.* 2003; **180**: 1375–8.
7 Maleux G, Nevens F, Heye S, Verslype C, Marchal G. The use of carbon dioxide wedged hepatic venography to identify the portal vein: comparison with direct catheter portography with iodinated contrast medium and analysis of predictive factors influencing level of opacification. *J. Vasc. Interv. Radiol.* 2006; **17**: 1771–9.
8 Debernardi-Venon W, Bandi J-C, Garcia-Pagán J-C *et al.* CO_2 wedged hepatic venography in the evaluation of portal hypertension. *Gut* 2000; **46**: 856–60.
9 Futagawa S, Fukazawa M, Musha H *et al.* Hepatic venography in noncirrhotic idiopathic portal hypertension. *Radiology* 1981; **141**: 303–9.
10 Scott J, Dick R, Long RG *et al.* Percutaneous transhepatic obliteration of gastro-oesophageal varices. *Lancet* 1976; **2**: 53–5.
11 Futagawa S, Fukazawa M, Horisawa M *et al.* Portographic liver changes in idiopathic noncirrhotic portal hypertension. *AJR Am. J. Roentgenol.* 1980; **134**: 917–23.
12 Kimura K, Tsuchiya Y, Ohto M *et al.* Single-puncture method for percutaneous transhepatic portography using a thin needle. *Radiology* 1981; **139**: 748–9.
13 Funaki B, Rosenblum JD, Leef JA *et al.* Percutaneous treatment of portal venous stenosis in children and adolescents with segmental hepatic transplants: long-term results. *Radiology* 2000; **215**: 147–51.
14 Stein M, Schneider PD, Ho HS, Eckert R, Urayama S, Bold RJ. Percutaneous transhepatic portography with intravascular ultrasonography for evaluation of venous involvement of hepatobiliary and pancreatic tumors. *J. Vasc. Interv. Radiol.* 2002; **13**: 805–14.
15 The Japan Society for Portal Hypertension. *The General Rules for Study of Portal Hypertension*, 2nd edn., 2004; 91–2.
16 Cho DR, Cho KJ, Hawkins IF Jr. Potential air contamination during CO_2 angiography using a hand-held syringe: theoretical considerations and gas chromatography. *Cardiovasc. Intervent. Radiol.* 2006; **29**: 637–41.
17 Kimura K, Ohto M, Matsutani S, Furuse J, Hoshino K, Okuda K. Relative frequencies of portosystemic pathways and renal shunt formation through the "posterior" gastric vein: portographic study in 460 patients. *Hepatology* 1990; **12**: 725–8.
18 Watanabe K, Kimura K, Matsutani S *et al.* Portal hemodynamics in patients with gastric varices: a study in 230 patients with esophageal and/or gastric varices using portal vein catheterization. *Gastroenterology* 1988; **95**: 434–40.
19 von Herbay A, Frieling T, Haeussinger D. Color Doppler sonographic evaluation of spontaneous portosystemic shunts and

inversion of portal venous flow in patients with cirrhosis. *J. Clin. Ultrasound* 2000; **28**: 332–9.
20 Anderson CM. GI magnetic resonance angiography. *Gastrointest. Endosc.* 2002; **55**: S42–8.
21 Taourel P, Blanc P, Dauzat M *et al.* Doppler Study of mesenteric, hepatic, and portal circulation in alcoholic cirrhosis: relationship between quantitative Doppler measurements and the severity of portal hypertension and hepatic failure. *Hepatology* 1998; **28**: 932–6.
22 Lin J, Zhou KR, Chen ZW, Wang JH, Yan ZP, Wang YX. 3D contrast-enhanced MR portography and direct X-ray portography: a correlation study. *Eur. Radiol.* 2003; **13**: 1277–85.
23 Madoff DC, Abdalla EK, Vauthey JN. Portal vein embolization in preparation for major hepatic resection: evolution of a new standard of care. *J. Vasc. Interv. Radiol.* 2005; **16**: 779–90.
24 Abulkhir A, Limonqelli P, Healey AJ *et al.* Preoperative portal vein embolization for major liver resection: a meta-analysis. *Ann. Surg.* 2008; **247**: 49–57.
25 Adani GL, Baccarani U, Risaliti A *et al.* Percutaneous transhepatic portography for the treatment of early portal vein thrombosis after surgery. *Cardiovasc. Intervent. Radiol.* 2007; **30**: 1222–6.
26 Shibata T, Itoh K, Kubo T *et al.* Percutaneous transhepatic balloon dilation of portal venous stenosis in patients with living donor liver transplantation. *Radiology* 2005; **235**: 1078–83.
27 Mizumoto H, Matsutani S, Fukuzawa T *et al.* Hemodynamics in the left gastric vein after endoscopic ligation of esophageal varices combined with sclerotherapy. *J. Gastroenterol. Hepatol.* 2001; **16**: 495–500.